Master's thesis

NTNU
Norwegian University of Science and Technology
Faculty of Natural Sciences
Department of Biotechnology and Food Science

Elise Borgen Holmås

Chitin-*b*-chitosan diblocks: preparation and characterization

Master's thesis in Biotechnology (MTKJ)
Supervisor: Bjørn E. Christensen
June 2022

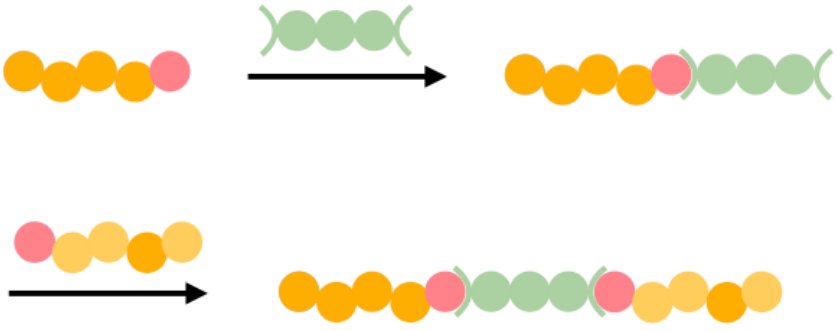

NTNU
Norwegian University of
Science and Technology

Elise Borgen Holmås

Chitin-*b*-chitosan diblocks: preparation and characterization

Masteroppgave i MTKJ
Veileder: Bjørn E. Christensen
Juni 2022

Norges teknisk-naturvitenskapelige universitet
Fakultet for naturvitenskap
Institutt for bioteknologi og matvitenskap

NTNU
Kunnskap for en bedre verden

Preface

This master thesis was conducted at the Department of Biotechnology and Food Science (IBT) at Norwegian University of Science and Technology (NTNU) between January and June 2022.

I hereby thank my supervisor Bjørn E. Christensen for giving me the opportunity to explore the growing field of diblock polysaccharides, and for his continuous guidance throughout the project. Moreover, I would like to thank Senior Engineers Wenche I. Strand and Olav A. Aarstad for technical assistance in the laboratory.

Lastly, I would like to thank my fellow master students Celine E. Eidhammer and Victor Zylla for great teamwork, discussions and environment.

The past five years are filled with unforgettable memories, to which NTNU has contributed enormously.

Trondheim, June 16, 2022

Elise Holmås

Abstract

The scope of this thesis was to prepare and characterize a chitin-*b*-chitosan diblock of the type A_nM-PDHA-MD_m. This included upscaling of A_nM oligomers based on a protocol by Mo *et al.* [22]. Due to their sustainability, biocompatibility and biodegradable nature, chitin and chitosan are very versatile for biomedical applications, specifically drug delivery systems and gene therapy. Here, the field of block polysaccharide structures is emerging rapidly, with an expanding set of applications. Being a polycation, chitosan has a complex-forming ability enabling it to associate with anionic structures. Chitin has adjuvanting effects and induces the production of cytokines and chemokines by a variety of cell surface receptors, like Toll-like receptor 2 (TLR-2), dectin-1 and macrophage mannose receptor. Combined, chitin-*b*-chitosan diblocks may be used to stabilize mRNA with adjuvanting effects in future vaccines, thus a protocol for their preparation is of high interest.

The preparation of the diblock comprised three main steps: preparation of A_nM -and D_nM oligomers by nitrous acid (HONO) degradation; preparation of A_nM-PDHA conjugates; and conjugation of D_mM to A_nM-PDHA. Upscaling A_nM oligomers was done by using high-capacity SEC columns for fractionation, and desalting pooled fractions by centrifugal filtration. Small-scale testing of centrifugal filtration by HPAEC-PAD using various polymer samples (HA, SBG, G_7, G_{20} and $Dext_{34}$) indicated that dimers were withheld by the filter. However, large-scale purification proved unsuccessful for oligomers with a DP < 10. When separating D_nM oligomers, NaAc was explored as an alternative to AmAc as the mobile phase to avoid direct self-branching by Schiff base reaction. However, loss of M unit due to self-branching was confirmed by ^{1}H-NMR, indicating that the reaction can take place at pH < pK_a which is lower than previously assumed.

A_4M was successfully conjugated with *O,O'*-1,3-propanediylbishydroxylamine (PDHA), followed by reduction with α-picoline boran (PB). For diblock preparation, in-house D_5M was used due to insufficient D_nM recovery. D_5M and A_4M-PDHA were conjugated in equimolar ratios and reduced as described for A_4M-PDHA. Purified diblock was characterized using ^{1}H-NMR, proving the conjugation was successful. Throughout the preparation of A_4M-PDHA-MD_5, significant loss of material was a recurring observation. It is therefore assumed that a MWCO = 3.5 kDa during dialysis was inappropriate for oligomers with a DP < 10, and the majority of the loss may have occurred here. A MWCO = 500-1000 Da resulted in a yield of 78.5% compared to < 3% for MWCO = 3.5 kDa when purifying A_4M-PDHA, further strengthening this assumption. However, in the preparation of D_nM oligomers, material could be lost inside the columns due to electrostatic interactions between chitosan and the stationary phase.

Sammendrag

Formålet med denne oppgaven var å lage og karakterisere en kitin-*b*-kitosan diblokk av typen A_nM-PDHA-MD_m. Dette inkluderte en oppskaleringsmetode for A_nM oligomerer basert på en protokoll fra Mo *et al.* [22]. Kitin og kitosan er svært anvendelige for biomedisinske formål grunnet deres bærekraftige, biokompatible og bionedbrytbare natur, da særlig innen transportsystemer for legemidler og genterapi. Strukturer av blokkpolysakkarider er et raskt voksende felt med økende bruksområder. Ettersom kitosan er et polykation, har den kompleks-dannende egenskaper med anioniske strukturer. Videre har kitin adjuvante egenskaper og induserer produksjon av cytokiner og kjemokiner gjennom en rekke overflatereseptorer, slik som Toll-lignende reseptor 2 (TLR-2), dektin-1 og makrofag mannose reseptor. Kombinert, kan kitin-*b*-kitosan diblokker benyttes til å stabilisere mRNA med adjuvante egenskaper i fremtidige vaksiner, så en protokoll er derfor av stor interesse.

Tillaging av diblokken kan deles inn i tre hoveddeler: preparere A_nM -og D_nM-oligomerer ved hjelp av salpetersyrling (HONO); preparere A_nM-PDHA konjugater; og konjugere D_mM til A_nM-PDHA. Oppskalering av A_nM-oligomerer ble gjort ved å bruke store SEC kolonner til fraksjonering, samt rense dem ved hjelp av sentrifugefiltrering. Testing av sentrifugefiltreringen i liten skala med ulike polymerer (HA, SBG, G_7, G_{20} og $Dext_{34}$) viste at filteret holdt tilbake dimerer. Dette ble tilbakevist i stor skala, hvorav oligomerer med DP < 10 gikk gjennom filteret. Ved SEC-fraksjonering av D_nM-oligomerer ble NaAc utforsket som et alternativ til AmAc som bruk av mobilfase, for å unngå selvforgreining ved Schiff basereaksjon. Tap av M-enheter som følge av selvforgreining ble likevel bekreftet ved ^{1}H-NMR, noe som tyder på at reaksjonen kan skje ved pH < pK_a. Dette er lavere enn tidligere antatt.

A_4M ble konjugert til *O,O'*-1,3-propanediylbishydroxylamine (PDHA), etterfulgt av redusering med α-picoline boran (PB). En tidligere D_5M-prøve ble brukt i tillagingen av A_4M-PDHA-MD_5, ettersom utbyttet av D_nM var utilstrekkelig. D_5M og A_4M-PDHA ble konjugert i ekvimolare mengder og redusert som beskrevet for A_4M-PDHA. Renset diblokk ble karakterisert ved hjelp av ^{1}H-NMR, noe som viste at konjugeringen var vellykket. Signifikante massetap var en gjennomgående observasjon i hvert steg av tillagingen av A_4M-PDHA-MD_5. På bakgrunn av dette antas det at en MWCO = 3.5 kDa er uegnet for oligomerer med en DP < 10, hvorav mesteparten av massetapet kan skyldes dialysen. En MWCO = 500-1000 Da ga et utbytte på 78.5% sammenlignet med < 3% for MWCO = 3.5 kDa ved rensing av A_4M-PDHA. Like fullt kan tap av D_nM-oligomerer forekomme i SEC-kolonnene på grunn av elektrostatiske interaksjoner mellom kitosan og den stasjonære fasen.

Abbreviations

A	*N*-acetyl-D-glucosamine
AcOH	Acetic acid
AmAc	Ammonium acetate
CHOS	Chitooligosaccharides
D	D-glucosamine
Dext	Dextran
DP	Degree of polymerization
DP_n	Number average degree of polymerization
F_A	Number of *N*-acetylglucosamine residues
F_D	Number of glucosamine residues
G	α-L-Guluronic acid
GlcNAc	*N*-acetyl-D-glucosamine
GlcN	D-glucosamine
HA	Hyaluronic acid
HMF	5-hydroxymethyl-2-furfural
^{1}H−NMR	Proton nuclear magnetic resonance
HONO	Nitrous acid
HPAEC-PAD	High-performance anion-exchange chromatography with pulsed amperometric detection
M	2,5-anhydro-D-mannose
MQ-water	Milli-Q water (ultrapure water)
MWCO	Molecular weight cut-off
NaAc	Sodium Acetate
$NaBH_3CN$	Sodium cyanoborohydride
PB	α-picoline borane
PCBC	Polysaccharide-containing block copolymers
PDHA	*O,O'*-1,3-propanediylboshydroxylamine
PEG	Polyethylene glycol
PES	Polyethersulfone
pK_a	Acid dissociation constant
RT	Room temperature
SBG	β(1,3)-glucan
SEC	Size exclusion chromatography

Contents

1 Introduction

1.1 Background

Green chemistry and the use of renewable resources is of the utmost importance to ensure a sustainable future. Today, biomass is a promising alternative to fossil fuels for the production of functional materials [37]. Biopolymers, specifically polysaccharides, are ubiquitous with a high structural diversity that provide a wide range of physical and chemical properties. They are inexpensive, biodegradable, biocompatible and non-toxic, enabling them to be used in various fields, such as biomedicine, material science and nutrition. Polysaccharides are stimuli-responsive and necessary for many biological processes, including regulation of cell growth, cell recognition and adhesion, inflammation and pathogenesis [25]. Chemical modifications of polysaccharides, such as lateral conjugation, usually change their properties. However, terminal conjugation at the reducing end preserves more of the intrinsic properties, resulting in novel types of polymer structures termed block polysaccharides. Diblock polysaccharides, comprising two constitutionally different oligo- or polysaccharide blocks, have the ability to form a variety of nanoscale structures [27]. This opens up new possibilities within biomedical applications, including drug delivery systems and non-viral vectors for gene therapy.

Chitin is a neutral homopolymer of GlcNAc (A) residues and the second most abundant polysaccharide in nature, occurring as crystalline microfibrils in the exoskeleton of crustaceans and insects, as well as the cell walls of yeast and fungi [29]. In the last decade, chitin has demonstrated complex effects on innate and adaptive immune responses, such as the ability to recruit and activate immune cells, as well as having adjuvanting effects. It induces the production of cytokines and chemokines by a variety of cell surface receptors, like Toll-like receptor 2 (TLR-2), dectin-1 and macrophage mannose receptor [16]. Chitosan is a polycationic heteropolymer derived from chitin by partial de-*N*-acetylation, and can form polyelectrolyte complexes (PEC) with negatively charged particles [30]. This property makes chitosan highly attractive for mRNA / siRNA delivery systems [33]. Preparation of chitin- and chitosan diblocks with dextran have successfully been reported [22,12]. Here, both chitin and chitosan oligomers were end-functionalized by 2,5-anhydro-D-mannose (M), which is a result of nitrous acid (HONO) depolymerization. The M residue render the oligomers highly reactive, thus making them ideal for diblock preparation. A_nM-*b*-MD_m diblocks have yet to be explored, and would be of great importance for adjuvanting mRNA-delivery systems due to the complex-forming ability and adjuvanting effect of chitosan and chitin, respectively.

1.2 Aim

The aim of this Master's thesis was to prepare and characterize chitin-*b*-chitosan diblocks. This comprised

- Explore a method for upscaling oligomer preparation, specifically A_nM.
- Prepare A_4M-PDHA and conjugate to D_5M.
- Develop a preparative protocol for chitin-*b*-chitosan diblocks.

A visualization of the aim is presented in Figure 1.2.1. Preparative protocols for chitin- and chitosan diblocks with PDHA-activated dextran have been successfully reported [22,12]. However, there is no protocol for the preparation of A_nM-PDHA-MD_m, with its chemical structure shown in Figure 1.2.2. By end-functionalizing both chitin and chitosan oligomers with an M residue, its high reactivity is exploited two folds, decreasing the preparation time. Thus, the development of such a protocol was of high interest, along with the characterization of a A_nM-PDHA-MD_m diblock.

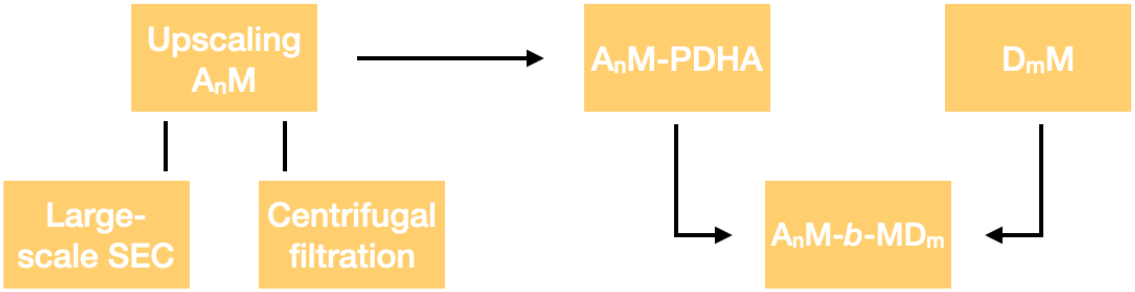

Figure 1.2.1: Overview of the aim of the Master's thesis: upscaling chitin oligomers (A_nM), and prepare and characterize chitin-*b*-chitosan diblocks.

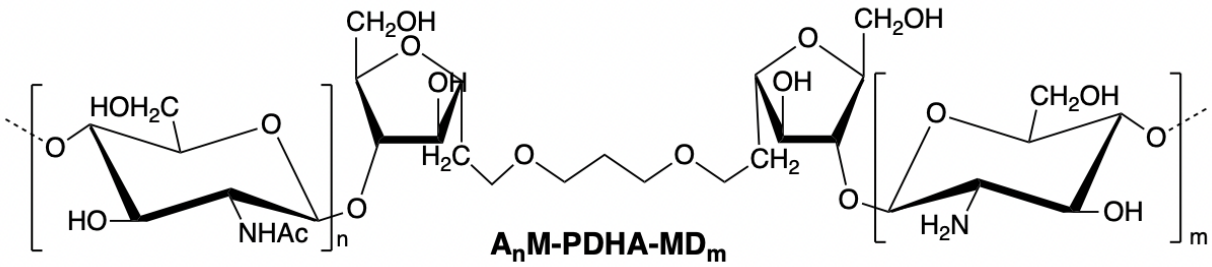

Figure 1.2.2: Chemical structure of a A_nM-b-MD_m diblock.

2 | Theory

This Master's thesis is a continuation of my specialization project carried out in the fall of 2021 [14], thus some of the theory overlap. Specifically, Section 2.3 is directly acquired from my specialization project, whereas Sections 2.4.1 2.4.3 are summarized in this thesis, but can be found in more detail in the project.

2.1 Block copolymers

Block copolymers comprise two or more terminally linked polymers, which are constitutionally different. In contrast to lateral linking, terminal linking results in new structures in which the intrinsic properties are preserved. A non-repeating molecule is typically used as a linker. They are described extensively in literature, varying from the most simple copolymer, a diblock (AB), to a star whose arms are blocks [26, 11]. An illustration of various block copolymers are shown in Figure 2.1.1.

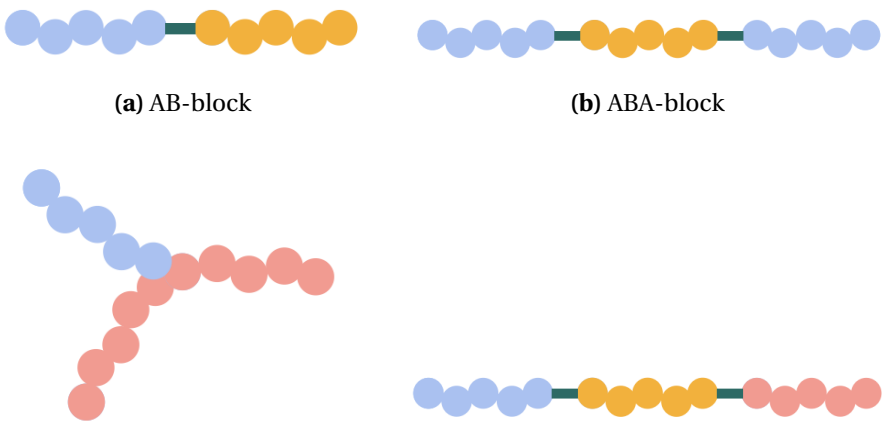

(a) AB-block **(b)** ABA-block

(c) Star-block **(d)** ABC-block

Figure 2.1.1: Schematic representations of various block copolymers comprising two or three constitutionally different and terminally linked polymers. **(a)** Diblocks, **(b)** triblocks and **(c)** star-blocks can be obtained from two polymers, while three polymers result in a different triblock **(d)**.

Synthetic block copolymers

Synthetic block copolymers, typically obtained from petroleum-based resources, are amphiphilic, comprising a hydrophobic and hydrophilic block. This enables them to self-assemble under appropriate conditions. Some examples include the self-assembly of AB or ABC block copolymers, in which they form various ordered structures such as micelles, polymersomes and lamellae that can be applied in many fields [2]. The strategy advances within block copolymers have made it possible to create complex structures, and it remains an active field of research [26]. Despite their simplicity, diblocks are the most studied as they can form a variety of nanoscale structures [27]. In recent years, the focus on sustainability and renewable resources has increased, resulting in a gradual shift from synthetic block copolymers to polysaccharide-containing block copolymers, and block polysaccharides.

Polysaccharide-containing block copolymers

Polysaccharides are involved in many biological processes. Among these are regulation of cell growth and inflammation by acting as attachment sites for hormones and infectious toxins, cell recognition and adhesion, as well as structural support [25]. Due to their biocompatible and structurally diverse nature, a wide range of applications can be obtained. Structurally, the large number of hydroxyl groups attached to polysaccharides indicate that they will have a low reactivity. However, the terminal residue exist in equilibrium between its open and closed ring form which is shown in Figure 2.1.2, albeit favoring the cyclical form. Chemical modifications are made possible by an electrophilic aldehyde group, present in the open chain form, that act as a reducing agent [45].

Polysaccharide-containing block copolymers (PCBC) represent a class of more sustainable alternatives to synthetic copolymers, and have been studied for decades [45]. They are used in emulsifiers and surfactants, and have the ability to self-assemble [11]. Here, the hydrophilic polysaccharide form a stable interphase with the aqueous phase, stabilizing the self-assembled hydrophobic polymer core. Various blocks have been described in literature, such as PEG-based copolymers attached to chitosan, hyaluronic acid (HA) and dextran [17]. These PCBC have shown potential as drug delivery systems and advanced biomaterials for tissue engineering, cell encapsulation and immunogenicity. Nevertheless, synthetic blocks may bioaccumulate and elicit immune responses due to not being fully biodegradable.

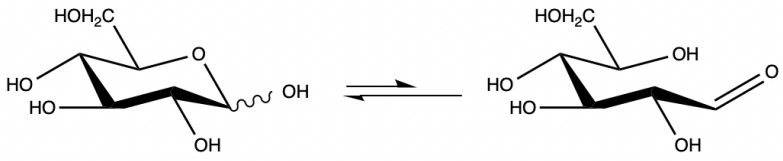

Figure 2.1.2: The open and closed stereoisomer of a glucose monomer. The reducing-end aldehyde of the open structure is available for further reactions.

Block polysaccharides

Block polysaccharides are a novel type of engineered block copolymers that exclusively comprise natural biopolymers. Due to their non-toxicity, they present beneficial properties compared to synthetic polymers, such as biocompatibility and biodegradability. Polysaccharides vary greatly with respect to structural composition, linkages and functional groups, enabling block preparation with specific properties valuable for biomedical applications. This includes self-assembling nanoparticles, which can be prepared from polysaccharides with intrinsic self-assembling properties (chitin, dextran, $\beta(1,3)$-glucans) and pH-dependent properties (HA, alginate, chitosan) [37]. One of the most common strategies for preparation of block polysaccharides is reducing end functionalization involving reductive amination, which is further described in Section 2.3. Distinct for chitosan is nitrous acid (HONO) degradation, forming chitooligosaccharides (CHOS) with a 2,5-anhydro-D-mannose (M) residue at the reducing end. This M-residue is highly reactive, resulting in faster diblock preparation [21], and is explained in Section 2.2.3.

2.2 Chitin and chitosan

2.2.1 Structure and chemical properties

Chitin, being the second most abundant polysaccharide in nature, occurs as crystalline microfibrils in the exoskeleton of crustaceans and insects, as well as the cell walls of yeast and fungi [29]. It is utilized where strength and reinforcement are required due to its structure and self-assembly properties. Chitin is a highly hydrophobic, unbranched homopolymer consisting of *N*-acetyl-D-glucosamine (GlcNAc, A) residues linked by $\beta(1,4)$-glucosidic bonds. Moreover, there are two main allomorphs, α-chitin and β-chitin, in which the respective chains are antiparallel and densely packed due to intra- and intermolecular hydrogen bonding, or parallel and less densely packed [4]. β-chitin is the most abundant form, and results in its insoluble nature in common solvents. However, chitin with a degree of polymerization (DP) < 10 is water-soluble, and special solvents such as DMAc/LiCl or cold alkali can also be used [22].

Pure chitin is rarely found in nature, and usually some of the GlcNAc residues are deacylated, resulting in D-glucosamine (GlcN, D) [39]. Chitin is therefore commonly described as a fraction of *N*-acetylated residues, F_A, described by Equation (2.2.1). Here, n_A and n_D represent the number of GlcNAc and GlcN residues respectively, whereas F_D is the fraction of GlcN. Partial de-*N*-acetylation of chitin results in chitosan with a varying degree of F_A, ranging between 0.10 and 0.20, and 0.9 and 1 for chitosan and chitin, respectively [22,18].

$$F_A = \frac{n_{GlcNAc}}{n_{GlcNAc} + n_{GlcN}} = \frac{n_A}{n_A + n_D} = 1 - F_D \tag{2.2.1}$$

The chemical structure of chitin and chitosan is shown in Figure 2.2.1. Unlike chitin, chitosan is polycationic due to the free amino group (NH_3^+) of the D residues, making it highly responsive to changes in pH and ionic strength. Due to amino groups being bases, they follow the equilibrium described by Equation (2.2.2). The pK_a is around 6.5, above which it is neutral and precipitates [47]. When pH < pK_a, the polycation exists in an expanded structure due to electrostatic repulsion between the amino groups, resulting in a high intrinsic viscosity. Highly de-*N*-acetylated chitosan (F_A between 0 and 0.2) are insoluble at neutral and high pH, whereas chitosan with F_A between 0.4 and 0.6 remain soluble at pH 7, as a result of the decreased possibility of neutral chains (with a high number of A residues) aligning [46,47]. This property enables chitosan to participate in a variety of applications, including mRNA and siRNA delivery, by interacting with the negative charges in DNA / RNA, forming polyelectrolyte complexes (PEC) [30].

$$-NH_3^+ \rightleftharpoons -NH_2 + H^+. \tag{2.2.2}$$

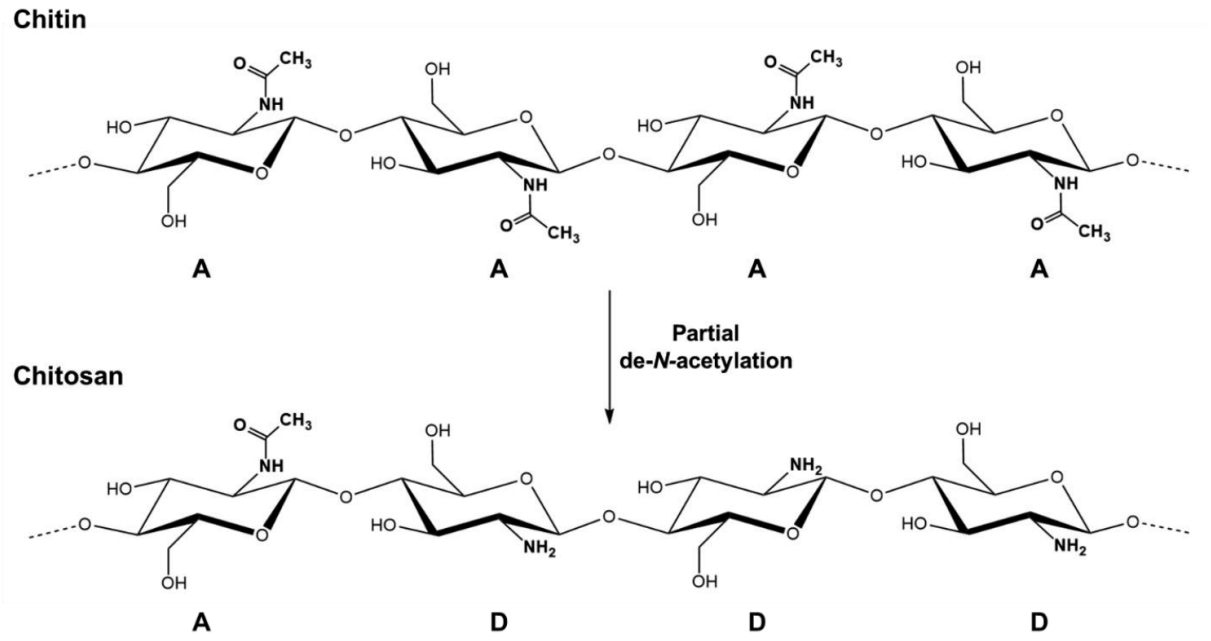

Figure 2.2.1: The chemical structure of chitin and chitosan. Chitin is a homopolymer comprising $\beta(1,4)$-linked *N*-acetyl-D-glucosamine (GlcNAc, A), while chitosan is a partially de-*N*-acetylated derivative consisting of D-glucosamine (GlcN, D) in addition to GlcNAc residues [21].

2.2.2 Chitooligosaccharides (CHOS)

Chitooligosaccharides (CHOS) are typically defined as chitosans with a DP < 20 (M_w < 4 kDa), and are obtained by chemical or enzymatical degradation of chitin or chitosan [22]. Compared to high-molecular weight chitosan, CHOS have unique properties such as higher water-solubility and lower viscosity in aqueous solutions. They are highly bioactive, with immunoregulatory and antioxidant effects, as well as being anti-inflammatory [28].

2.2.3 HONO depolymerization of chitosan

HONO depolymerization of chitosan only affects the unacetylated D residues and converts them into 2,5-anhydro-D-mannose (M) residues by deamination, followed by chain scission. This results in a mixture of CHOS with an M residue at the reducing end (A_nM and D_nM) as shown in Figure 2.2.2. Here, *n* refers to the number of A or D residues, in which the degree of polymerization will be DP = n + 1. By having HONO in excess or limited amounts, A_nM or D_nM are obtained, respectively. Because A residues remain unaffected, the reaction is first order with respect to the concentrations of HONO and D residues, where the molar ratio of HONO to deamination is 1:1 [3]. The rate of depolymerization is independent of the molecular weight, thus the degree of scission (α) is governed by the HONO concentration and F_D.

The mechanism for HONO degradation of chitosan is presented in Figure 2.2.3, where the main and alternative path comprise four and five steps, respectively. Nevertheless, the first two steps are shared. First, an unstable *N*-nitrosamine is formed due to the amino group of a D residue being attacked by an acidium ion ($NH_2O_2^+$), which is the result of protonated HONO. Subsequently, *N*-nitrosamine rearranges to form an unstable diazonium ion, releasing water. In the main path, the release of nitrogen by heterolysis results in a carbonium ion that is attacked by the ring oxygen. Further, the formation of a furanose with a pending aldehyde at C1 and the breaking of the glycosidic bond occur simultaneously, resulting in an M residue at the new reducing end [49, 9, 34]. For the alternative deamination mechanism, the carbonium ion is attacked by C4 forming a furanose residue with the pending aldehyde at C2. However, the glycosidic linkage is not cleaved in this step, but can undergo acid hydrolysis to from the new reducing end [49, 9, 34].

The M-unit has been proven to make the oligomers particularly reactive due to its pending aldehyde [43], compared to the pyranose reducing end residues. This property has exploited in end-functionalization of precursors for chitin- and chitosan containing diblocks [43, 22, 12]. There are no by-products of nitrous acid depolymerization, however, if the M residue degrades, it forms 5-hydroxymethyl-2-furfural (HMF) when the pending aldehyde reacts with the unprotonated amino group of a D residue. HMF is a common by-product of Millard browning. This reaction occurs when the pH > pK_a, and forms a Schiff base. Further, acid catalyzed elimination remove water and the chain is cleaved, resulting in HMF and a normal reducing end (A or D). This illustrates the pH-dependency of the M residue degradation, which can be avoided by maintaining a low pH. [43].

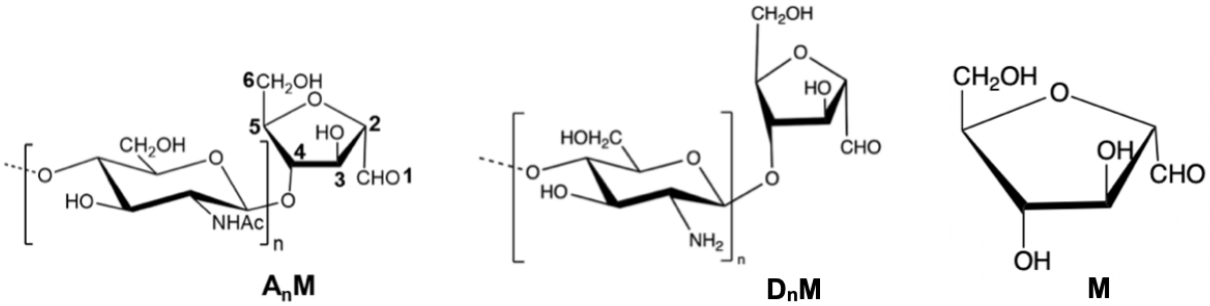

Figure 2.2.2: Chemical structures of nitrous acid depolymerized chitosan (A_nM and D_nM) and 2,5-anhydro-D-mannose (M).

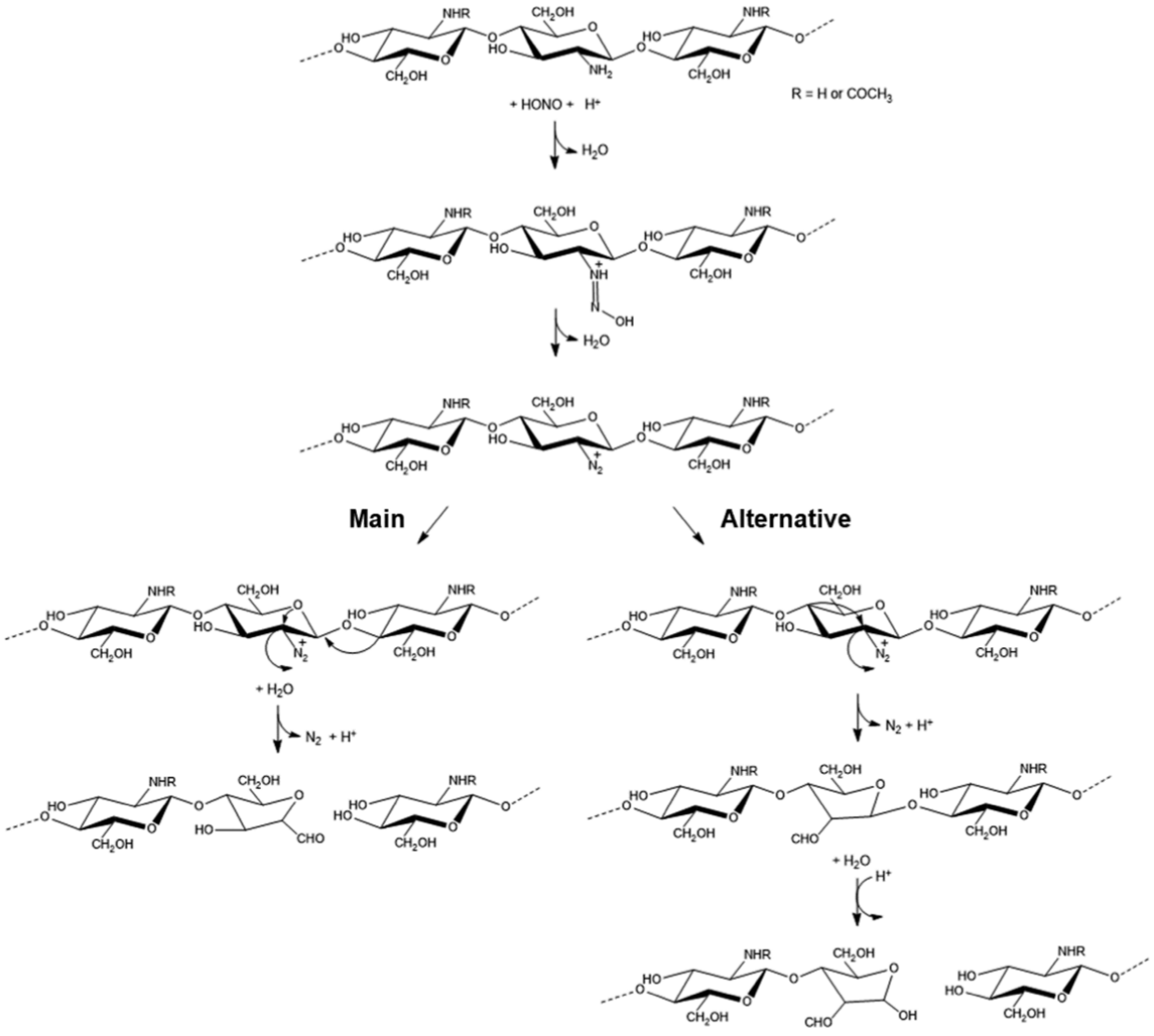

Figure 2.2.3: The main reaction shows the mechanism for nitrous acid (HONO) depolymerization of chitosan, while the alternative reaction shows the deamination mechanism resulting in chain scission following acid hydrolysis [21].

2.2.4 Biomedical applications

Because chitosan and chitin are biocompatible, biodegradable, non-toxic as well as renewable, they are of high interest within various fields such as biomedicine, material science, and food and nutrition. The applications of chitin are often limited by its low solubility in water, whereas chitosan is soluble under acidic conditions. However, high-molecular weight chitosan has a high viscosity in dilute acidic conditions. CHOS show increased water-solubility for both chitin and chitosan, hence being of increased interest.

Chitin- and chitosan based materials have been explored as substitutes within tissue engineering due to their antibacterial and antifungal properties. Vandevord *et al.* [44] studied the biocompatibility of chitosan scaffolding in mice. They found that although there was a large migration of neutrophils into the implantation area, there were minimal signs of inflammatory reactions to the material itself. Further, a novel asymmetric chitosan membrane was designed by Mi *et al.* [20] for wound dressing, showing an increased healing rate as well as a reduction in scar tissue formation. There are also studies exploring the use of chitosan for controlled drug release [5], such as anticancer and antimetastasis agents [13,28]. Here, bioactive molecules were associated to chitosan through various mechanisms, including ionic- and chemical crosslinking and ionic complexation, forming colloidal particles [28]. As for gene therapy, the polycationic nature of chitosan results in DNA condensation, whereby genes of interest can be transferred to target cells [42].

2.3 Reductive amination by oxime click reactions [14]

Reductive amination is a chemical process in which aldehydes react with amines, oxy-amines or hydrazides to form imines, oximes and hydrazones, also referred to as Schiff bases. Subsequently, these bases are irreversibly reduced to stable, secondary amines by a selective reducing agent [23], as shown in Figure 2.3.1. Reductive amination is acid-catalyzed, protonating the carbonyl oxygen of the aldehyde, and making it susceptible to a nucleophilic attack by the amine. Elimination of water results in the formation of imine in a mixture of (*E*) and (*Z*) isomers. An (*E*)-isomer is defined as two groups of high priority being attached to opposite sides of the C-N double bond, while a (*Z*)-isomer have the groups on the same side [38]. The tautomeric mixture is also in equilibrium with cyclic *N*-glucosides [23]. An exception to this, is reductive amination with nitrous acid degraded chitin or chitosan oligomers, where only (*E*)/(*Z*)-oximes are formed [21].

Oxime click reactions take advantage of the high nucleophilicity of oxiamines compared to amines, as they conjugate efficiently to the reducing end of carbohydrates [23]. Here, oximes are reversibly formed by reacting an aldehyde with an aminooxy group, resulting in a tautomeric mixture of (*E*)/(*Z*)-oximes, as well as *N*-pyranosides. Due to the low basicity of oxyamines, oximes can be formed under mildly acidic conditions, making them suitable for conditions where high molecular weight polymers are soluble. They also increase the hydrolytic stability of the formed oximes [27].

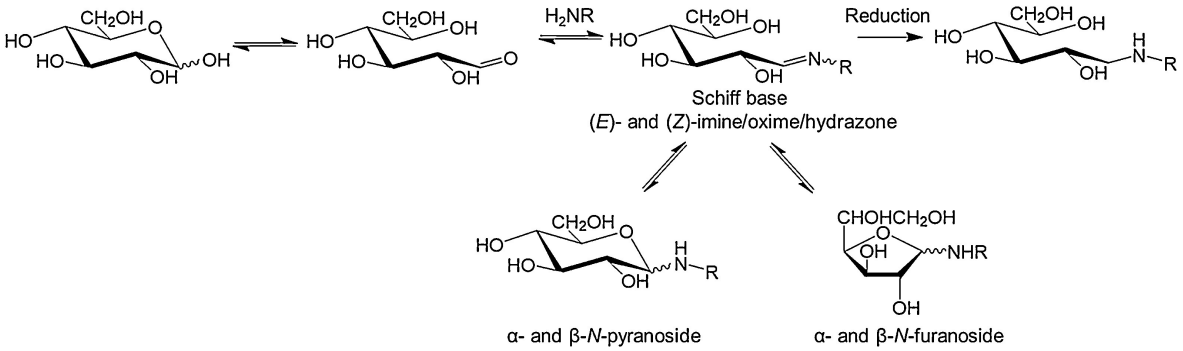

Figure 2.3.1: Reductive amination of a free aldehyde at the reducing end of glucose (used as an example). The aldehyde reacts with an amine-group forming Schiff bases in an (*E*)/(*Z*)-conformation mixture, in equilibrium with cyclic *N*-glycosides. Subsequent reduction form stable secondary amines [23].

2.3.1 *O,O*'-1,3-propanediylbishydroxylamine (PDHA) as a linker

O,O'-1,3-propanediylbishydroxylamine (PDHA), visualized in Figure 2.3.2a, is a symmetrical molecule with reactive oxyamine groups at both ends of a three-carbon backbone, making it ideal for cross-linking oligosaccharides. It has previously been used to activate chitooligosaccharides in preparation of chitin-*b*-dextran diblocks [22,23]. The terminal amino groups has a pK_a of 4.2, rendering PDHA positively charged at pH values under this. [23].

2.3.2 α-picoline boran (PB) as a reducing agent

In order to convert imines formed during conjugation into stable secondary amines, a reducing agent is required. It is important that the reducing agent has a high selectivity towards the imines. α-picoline boran (PB), shown in Figure 2.3.2b, is an aromatic reducing agent that is relatively new in the use of reductive amination of polysaccharides. It is a less hazardous and more sustainable choice to more traditional reducing agents such as sodium cyanoborohydride ($NaBH_3CN$) [6]. PB is applicable in different solvents, including water; is stable up to 150°C; has a high selectivity and low cost; and most importantly, generates no toxic waste [6]. This makes PB very beneficial for reactions involving polysaccharides.

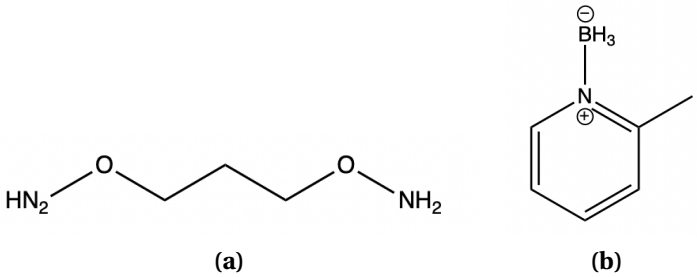

Figure 2.3.2: The chemical structure of O,O'-1,3-propanediylbishydroxylamine (PDHA) and α-picoline boran (PB), shown in **(a)** and **(b)** respectively.

2.4 Analytical methods

2.4.1 Size-Exclusion Chromatography (SEC)

This section highlights the main principles of SEC, in which the full text can be found in my specialization project [14].

Size-exclusion chromatography (SEC) is a type of high pressure liquid chromatography (HPLC) technique, in which molecules are separated according to their hydrodynamic volume when passing through a stationary phase of uniform porous particles [15]. The principles of SEC are visualized in Figure 2.4.1. Separation is achieved due to differential pore permeation, where low-molecular-weight components penetrate into the pores, while high-molecular-weight compounds are too large to elute in the void volume of the column, V_0, thus having a shorter retention time.

SEC is a relative M_w-technique, so it is important to calibrate the columns with an appropriate polymer standard of known molecular weight, such as dextran or polystyrene. The separation quality is affected by the column length, choice of material and the flow rate of the mobile phase through the system, and it can be improved by having multiple columns connected in series [24]. The most common signal detectors are refractive index, UV or fluorescence detectors, in which the data is plotted against the elusion volume or retention time, creating a chromatogram.

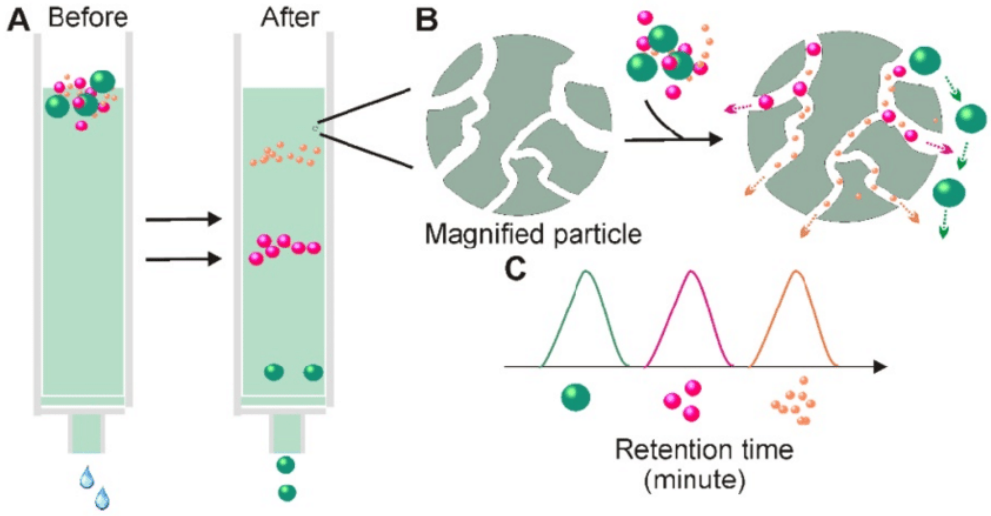

Figure 2.4.1: The principles of size-exclusion chromatography (SEC) that allows molecules to be separated by hydrodynamic volume. A sample solution is passed through a stationary phase of porous particles (A) where small molecules will enter the pores, thus having a greater retention time than large molecules, which elute in the void volume (B). This allows for a chromatogram to display the retention time and visualize the separation (C) [50][14]

2.4.2 High-performance anion-exchange chromatography with pulsed amperometric detection (HPAEC-PAD)

High-performance anion-exchange chromatography with pulsed amperometric detection (HPAEC-PAD), is a form of HPLC, just like SEC. However, it is an improved chromatographic technique for carbohydrate separation that takes advantage of their weakly acidic nature [31]. It allows for direct quantification of non-derivatized polysaccharides at low concentrations and high pH, with minimal preparation and cleanup necessary [19]. The high specificity towards carbohydrates is due to the pulsed amperometry only detecting compounds containing oxidizable functional groups at the detection voltage. Furthermore, neutral or cationic components elute in (or close to) the void volume, thus do not interfere with the analysis [31].

Ion-exchange chromatography separates ionic and polar compounds using columns containing positively or negatively charged functional groups opposite of the analytes. Thus anion-exchange columns, separating anions, are derivatized with positively charged functional groups, and visa versa for cation-exchange columns. The technique has been widely used when analyzing mono- and oligosaccharides, as well as amino acids, nucleotides, organic acids, and other polar molecules [32]. Analyte ions and eluent ions compete to bind to the surface of the stationary phase, thus separation occurs due to the repeated adsorption and desorption by the analyte and eluent ions, respectively.

PAD is a powerful detection method that requires no sample derivatization. At high pH, polysaccharides are electrocatalytically oxidized at the surface of a gold electrode by applying a positive potential, in which the current is proportional to the polysaccharide concentration [10]. Sodium hydroxide (NaOH) is typically used as the eluent. When a single potential is applied to the electrode, oxidation product cause electrode fouling resulting in a loss of analyte signal. A series of potentials that are applied for fixed time periods, called a waveform, is used to clean and restore the electrode surface for subsequent detection [32]. Several waveforms are used when analyzing different molecules in order to increase detection sensitivity and reduce sensitivity to baseline drift, dissolved oxygen and loss of electrode surface. An Ag/AgCl reference electrode is usually used as a half electrode [10].

2.4.3 Proton nuclear magnetic resonance (^{1}H-NMR) spectroscopy

This section is a summary of the main principles of ^{1}H-NMR spectroscopy, where the full text can be found in my specialization project [14].

Nuclear magnetic resonance (NMR) spectroscopy is a non-destructive analysis method used to elucidate both composition and structure of organic compounds. When in a magnetic field, under appropriate conditions, a sample can absorb electromagnetic radiation due to the magnetic properties of nuclei. The quantum spin number, I, determines the number of orientations a nucleus may have in an external magnetic field, and may have values of 0, 1/2, 1, 3/2 etc. with 0 representing no spin. It is dependent on both the atomic mass and number of the nuclei. One of the most widely used nuclei is ^{1}H, which has an I equal to 1/2. Following Equation (2.4.1), there are two possible energy states, one upper and one lower [36].

$$\text{Number of orientations} = 2I + 1 \tag{2.4.1}$$

When the ^{1}H nuclei is excited to a higher energy state, radiation is absorbed and released when they return to equilibrium. This release of radiation is recorded as resonance signals, providing a spectrum of chemical shifts, δ, in ppm (10^{-6}) for the respective protons. Electrons have a shielding effect on protons, thus resulting in various chemical shifts depending on the electron density around the protons [36]. Spin-spin coupling is a phenomenon where intervening bonding electrons cause peak splitting. Here, the state of an individual spin in a pair is affecting the energy associated with the other spin, thus the resonance frequency is altered. The peak will then appear as a doublet. If there are coupling between several proton spins, multiple peaks will appear. However, their chemical shift will be in the center between the peaks. Where there is no coupling, equivalent protons appear as a single peak, called a singlet [36].

^{1}H-NMR spectra and chemical shifts for CHOS

^{1}H-NMR is frequently used to characterize polysaccharides, despite the clustering of proton resonances around 3.4-4.0 ppm. It shows the anomeric protons in α- and β-configur-ations in the chemical shifts 5.1-5.8 ppm and 4.3-4.8 respectively [51]. Based on the intensities of the peak integrals of the H1 reducing end and H1 non-reducing end, the degree of polymerization (DP) can be determined, as described by Equation (2.4.2).

$$\text{DP} = \frac{\text{H1, non-reducing end}}{\text{H1, reducing end}} \tag{2.4.2}$$

^{1}H-NMR characterization for CHOS and nitrous acid depolymerized CHOS have previously been done [43, 40], in which the chemical shifts for proton resonances of the trisaccharides AAA, DDD, AAM and DDM are presented in Table 2.4.1. ^{1}H-NMR spectra of AA and DD are presented in Figure 2.4.2, while spectra of AAM and DDDM are shown in Figure 2.4.3.

Table 2.4.1: Chemical shifts for proton resonances of chitin (fully *N*-acetylated, AAA) and chitosan (fully de-*N*-acetylated, DDD) [40], and AAM and DDM obtained by nitrous acid degradation of chitin and chitosan, respectively [43]. All samples were dissolved in D_2O and chemical shifts were reported as ppm from TSP. AAM and DDM were characterized at 25°C, pH* 5.0 and 43°C, pH* 5.7, respectively.

Residue	H1	H2	H3	H4	H5	H6a	H6b	CH_3, Ac
A (α)	5.20	3.86	3.88	3.63	3.89	3.68	3.80	2.05
A (β)	4.72	3.69	3.66	3.62	3.52	3.67	3.84	2.05
A (non-reducing)	4.60	3.75	3.58	3.47	3.48	3.73	3.92	2.07
A (internal)	4.60	3.79	3.74	3.65	3.56	3.66	3.85	2.07
D (α)	5.44	3.34	4.03	3.88	4.04	3.77	3.84	-
D (β)	4.96	3.03	3.86	3.71	3.88	3.75	3.94	-
D (non-reducing)	4.84	3.12	3.69	3.49	3.55	3.76	3.95	-
D (internal)	4.87	3.16	3.88	3.74	3.94	3.76	3.95	-
M (AAM)	5.01	3.76	4.35	4.13	3.98	3.43	3.49	-
M (DDM)	5.09	3.84	4.44	4.22	4.13	n.d	n.d	-
Schiff base (DDM)	7.93-7.97	-	-	-	-	-	-	-

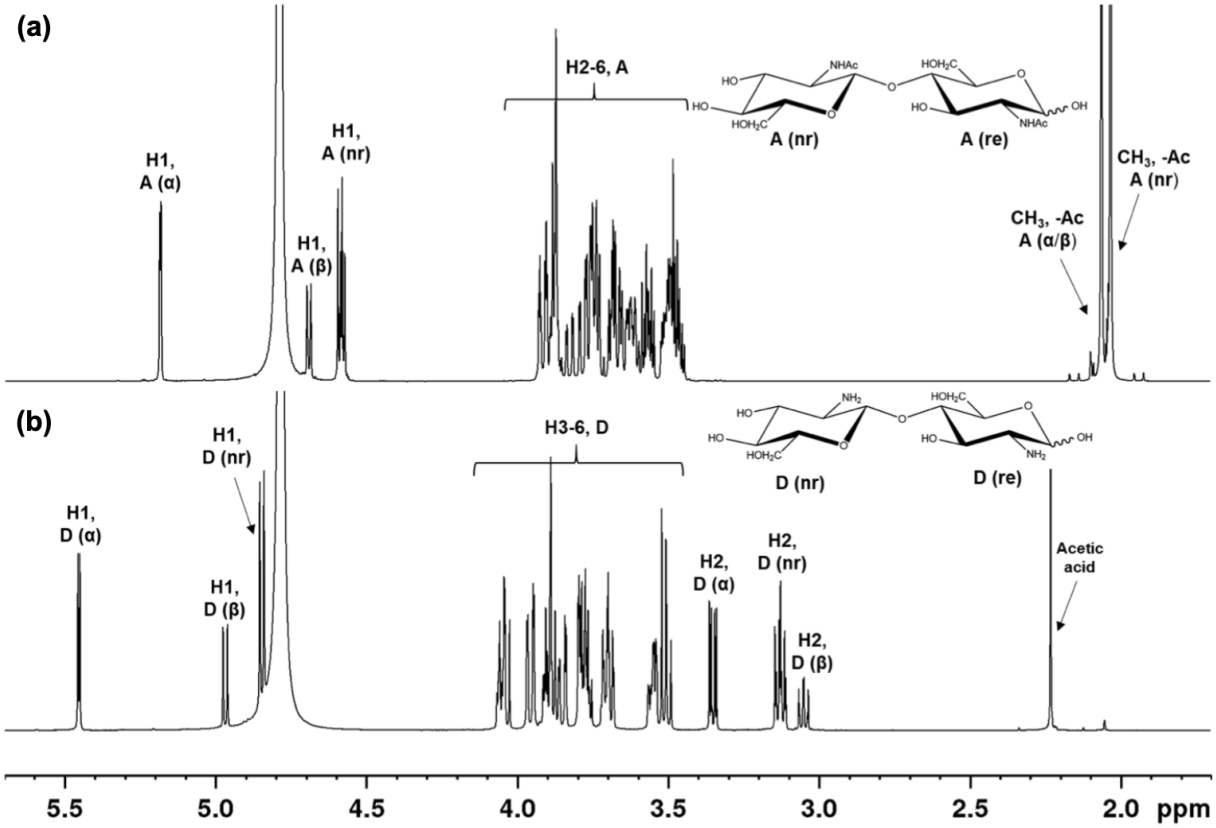

Figure 2.4.2: ^{1}H-NMR spectra of **(a)** AA and **(b)** DD in D_2O. The spectra are obtained from the PhD thesis of Ingrid V. Mo [21].

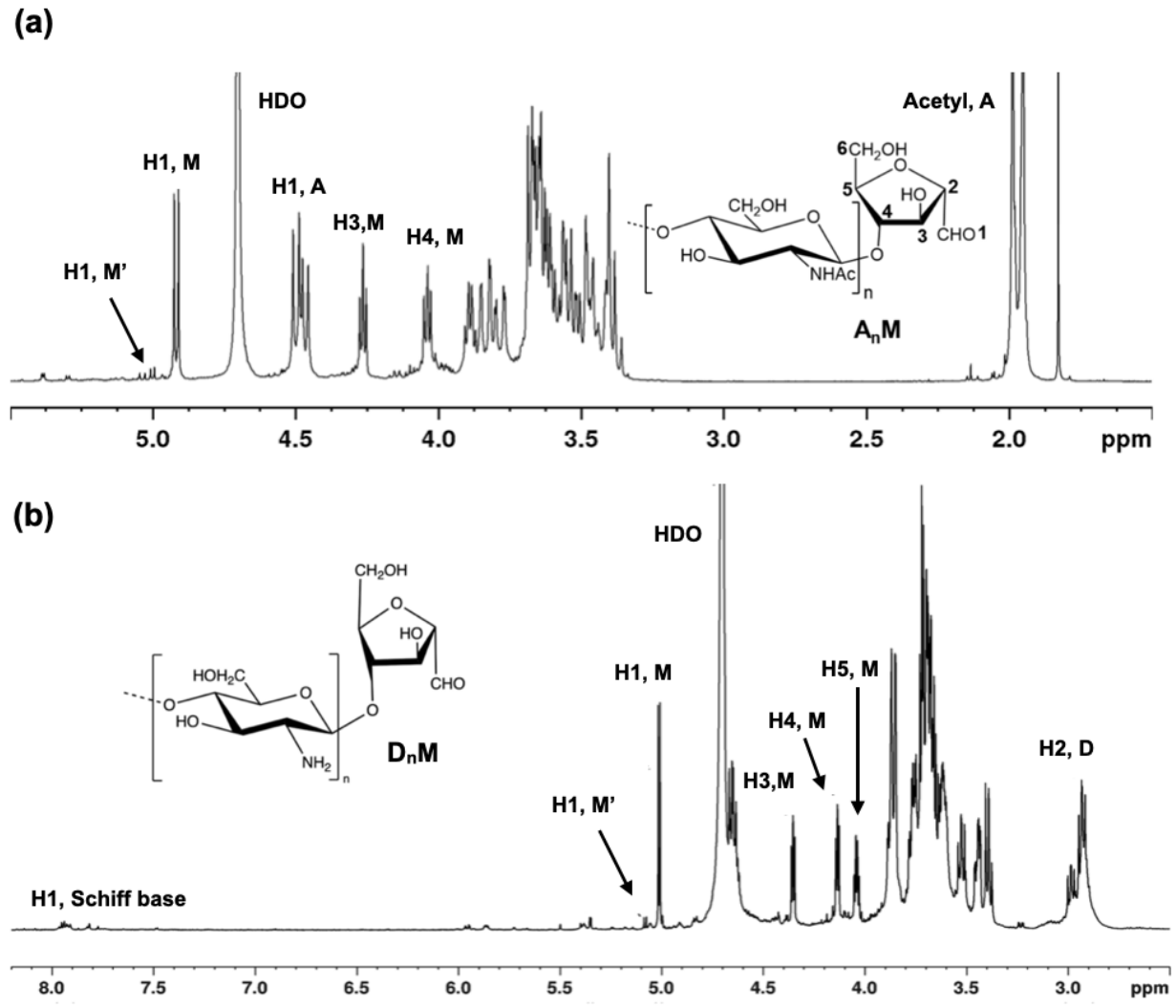

Figure 2.4.3: ^{1}H-NMR spectra (600 MHz, RT, D_2O) of **(a)** AAM and **(b)** DDDM (pH* 6.0). The spectra are obtained from Mina Gravdahl and Ingrid V. Mo, respectively [12,21].

3 Materials and methods

3.1 Materials

High molecular weight chitosan (F_A = 0.002 and F_A = 0.48) were obtained from an in-house sample and Advanced Biopolymers AS [11], respectively. *O,O'*-1,3-propanediylbis-hydroxylamine (PDHA) and α-picoline boran (PB) were purchased from Sigma-Aldrich. All other chemicals were obtained from commercial sources and were of analytical grade. Centricon Plus-70 centrifugal filter devices were obtained from Millipore.

3.2 SEC fractionation

3.2.1 System 1: small scale fractionation

For small-scale fractionation, a system comprising three Superdex 30 columns (HiLoad 26/60, GE Healthcare Bio-Science) in series, eluting NaAc or AmAc buffer (0.1 M or 0.15 M, pH 4.5, 0.8 mL/min) was utilized. Samples (4-200 mg) were dissolved in buffer (5 mL) and filtered (0.45 µm) before being injected into the system. A refractive index (RI) detector (Shodex RI-101) was used to monitor the separation, and fractions were collected by a fraction collector (LKB 2211 SuperRac), and pooled according to elusion times. Fractions were dialyzed (MWCO = 100-500 Da or 3.5 kDa) against MQ-water until measured conductivity was < 2 µS/cm and freeze-dried.

3.2.2 System 2: large-scale fractionation

Large-scale fractionation was obtained using a system composed of two Superdex 30 columns (BPG 140/950, GE Healthcare Bio-Science) in series. The mobile phase was AmAc buffer (0.15 M, pH 4.5), with a flow rate of 20 mL/min. Samples (3-10 g) were filtered (0.7 µm) prior to injection. To monitor the separation, the same RI detector from system 1 was utilized. Fractions were collected using a fraction collector (SuperFrac, Amersham Bioscience), pooled according to elusion times and either purified by dialysis (MWCO = 3.5 kDa), freeze-drying or centrifugal filtration (MWCO = 3.0 kDa), the latter being further described in Section 3.4.

3.3 HPAEC-PAD analysis

All HPAEC-PAD analyses were performed on a Dionex ICS 5000+ system (Thermo Scientific) with a 4x250 mm IonPac ASA4 main column and 4x50 mm AG4A guard column, by Senior Engineer Olav A. Aarstad (Department of Biotechnology, NTNU).

3.3.1 Alginate and hyaluronic acid oligomers

Samples of G_7, G_{19} and acid hydrolyzed HA oligomers were eluted at 24°C with isocratic NaOH (0.1 M) and a linear NaAc gradient (8.75 mM/min) for 100 minutes, with a flow rate of 1 mL/min. Further, a 15 minute equilibration step with NaOH (0.1 M) and NaAC (10 mM) was included. Samples were dissolved in MQ water to a concentration of 0.2 - 1 mg/mL before injection (25 µL). Partially acid hydrolyzed polyM (F_G = 0.0) and G block(F_G = 0.94) were used as standards. Waveform A (Gold-Ag-AgCl Re, Carbo, quad) was used for detection, and data were collected and processed with Chromeleon (Thermo Scientific) 7.2 software.

3.3.2 Dextran and β(1,3)-glucan oligomers

Samples of $Dext_{34}$ and acid hydrolyzed SBG were eluted at 24°C with isocratic NaOH (0.1 M) and a linear NaAc gradient (10-610 mM/min and 10-260 mM/min for dextran and SBG, respectively) for 90 minutes, where the flow rate was 1 mL/min. Further, a 15 minute equilibration step with NaOH (0.1 M) and NaAC (10 mM) was included. Like alginate and HA, samples were dissolved in MQ water to a concentration of 0.2 - 1 mg/mL before injection (25 µL). Here, a mixture of SBG with DP 2-6 was used as standards. Waveform A (Gold-Ag-AgCl Re, Carbo, quad) was used for detection, and data were collected and processed with Chromeleon (Thermo Scientific) 7.2 software.

3.4 Centrifugal filtration

Centrifugal filtration is commonly used in protein recovery for purifying and concentrating solutions, and was explored as an alternative to dialysis and evaporation. This was done in collaboration with fellow Master's students Celine E. Eidhammer and Victor Zylla Fæsther. Small-scale testing (10 mL) was done using two different membrane materials, regenerated cellulose (Amicon ultra-15) and polyethersulfone, PES (Sartorius, Vivaspin 20), where the MWCO was 3 kDa for both. Samples (1 mg/mL) of hyaluronic acid (HA, DP = 10), β(1,3)-glucan (SBG, DP = 10), $Dext_{34}$ and alginate G-blocks (DP = 7 and 20) were centrifuged (3500-4000 rcf, 25-70 min). In order to study the MWCOs, samples prior to and after filtration were analyzed using HPAEC-PAD as described in Section 3.3.

Large-scale filtration was used when purifying SEC fractions from system 2. Here, Centricon® Plus-70 centrifugal filters (Millipore, MWCO = 3 kDa) were used. The basic principles are visualized in Figure 3.4.1. Fractions were concentrated from 70 mL to 1 mL, diluted with MQ-water (10 mL) to further remove salt, and centrifuged (3500 rcf, 40 and 10 min for concentration and desalting, respectively). When recovering samples from the filter cup, a concentrate cup was used to spin them down (1000 rcf, 2 min). All centrifugation was done using an Allegra X-15R (Beckman Coulter) centrifuge equipped with a SX4750A rotor.

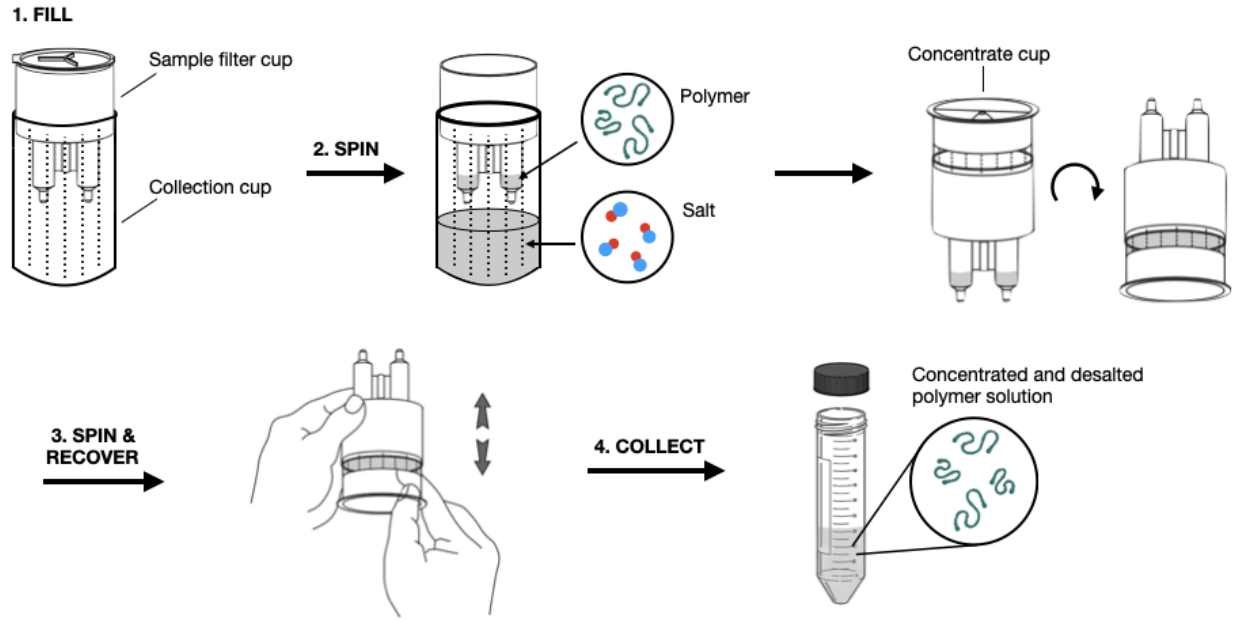

Figure 3.4.1: The principles of centrifugal filtration using Centricon® Plus-70 centrifugal filters (MWCO = 3 kDa, Millipore) [35]

3.5 Characterization by ^{1}H-NMR spectroscopy

For ^{1}H-NMR characterization, samples (2-5 mg) were dissolved in D_2O (475-500 µL) and transferred to 5mm NMR tubes. The NMR experiments were carried out on a Bruker Ascend NEO 600 MHz spectrometer (Bruker BioSpin AG, Fällanden, Switzerland) equipped with Avance III HD electronics, and a 5 mm Z-gradient CP-TCI cryogenic probe. Characterization was performed by obtaining 1D ^{1}H-NMR spectra at RT. TopSpin 4.1.3 software (Bruker BioSpin) was used to record, process and analyze all of the spectra.

3.6 Preparation of A_nM -and D_nM oligomers

The protocols for A_nM and D_nM preparation were obtained from the PhD thesis of Ingrid V. Mo [21] and Master's thesis of Mina Gravdahl [12], respectively. Based on these a method for up-scaling A_nM oligomers was explored. Chitosan (F_A = 0.48, 20 g and F_A < 0.002, 800 mg for A_nM and D_nM, respectively, 20 mg/mL) were dissolved in degassed MQ water containing AcOH (2.5 vol%) for 15-20 min using N_2, and left on a magnetic stirrer overnight at RT. The polymer solutions were then cooled to 4°C. Freshly prepared and degassed $NaNO_2$ solutions (1.3 and 0.25 molar ratio to D-units for A_nM and D_nM, respectively, 20 mg/mL) were cooled to 4°C before mixing, and left on a magnetic stirrer overnight in the dark.

The A_nM degradation mixture was centrifuged using a Thermo Scientific Sorvall Lynx 6000 centrifuge (10 000 rcf, 10 min). The pellet was washed with AcOH (2.5 vol%) three times to remove insoluble chitin oligomers. The supernatant, containing water-soluble chitin oligomers, was filtered (2.7 and 0.7 µm), fractionated using SEC system 2 and purified, as described in Section 3.2.2.

The D_nM degradation mixture was directly freeze-dried and dissolved in buffer (20 mg/ mL, 0.1 M NaAc, pH 4.5) prior to SEC fractionation using system 1. NaAc was removed by dialysis (MWCO = 3.5 kDa) against pH-adjusted (pH 4.5) and normal MQ-water until the conductivity was < 2 µS/cm. Selected fractions of both A_nM and D_nM were freeze-dried and characterized by ^{1}H-NMR spectroscopy as explained in Section 3.5.

3.7 Preparation of PDHA-activated A_nM

A_4M (20.5 mM) was conjugated with 10x PDHA (205) in NaAc buffer (pH 4.0, RT) for 5 hours before reduction with 20x PB (410 mM) for 48h at 40°C. The reduction was terminated by dialysis (MWCO = 500-1000 Da and 3.5 kDa) against NaCl (0.05 M) until the remaining PB was removed, followed by MQ-water until the conductivity was < 2µS/cm. Subsequently, the reaction mixture was fractionated using SEC system 1, freeze-dried and characterized by ^{1}H-NMR spectroscopy.

3.8 Preparation of A_4M-*b*-MD_5 diblocks

For diblock preparation, A_4M-PDHA and an in-house D_5M sample, prepared by Jesper E. Pedersen (Department of Biotechnology, NTNU), were conjugated in equimolar ratios (8.0 mM) in NaAc buffer (pH 4.0, RT) for 5 hours. Subsequently, conjugates were reduced with 20x PB (160 mM) at 40°C for 48h and dialyzed (MWCO = 3.5 kDa) against NaCl (0.05 M) until PB was dissolved, followed by MQ water until the conductivity was < 2µS/cm. Reacted and unreacted products were separated using SEC system 1, purified by dialysis and freeze-dried for further ^{1}H-NMR characterization.

4 | Results

Preparation of chitin-*b*-chitosan diblocks consisted of three main parts, illustrated in Figure 4.0.1. In the first part, A_nM and D_nM oligomers were obtained by nitrous acid degradation, fractionated by SEC, purified, and characterized by ^{1}H-NMR. Here, the protocol for A_nM oligomers developed by Mo *et al.* was used. D_nM preparation was done in collaboration with Master's student Celine E. Eidhammer, following a protocol developed by Gravdahl *et al.*. In part two, A_4M oligomers were activated with PDHA, reduced with PB, purified and characterized. Part three comprised attaching D_5M to A_4M-PDHA, resulting in A_4M-PDHA-MD_5 diblocks. Additionally, a method for upscaling oligomer preparation was developed in collaboration with Celine E. Eidhammer and Victor Zylla Fæster. Here, centrifugal filtration was explored as a time-saving alternative to evaporation and dialysis for sample concentration and desalting, respectively.

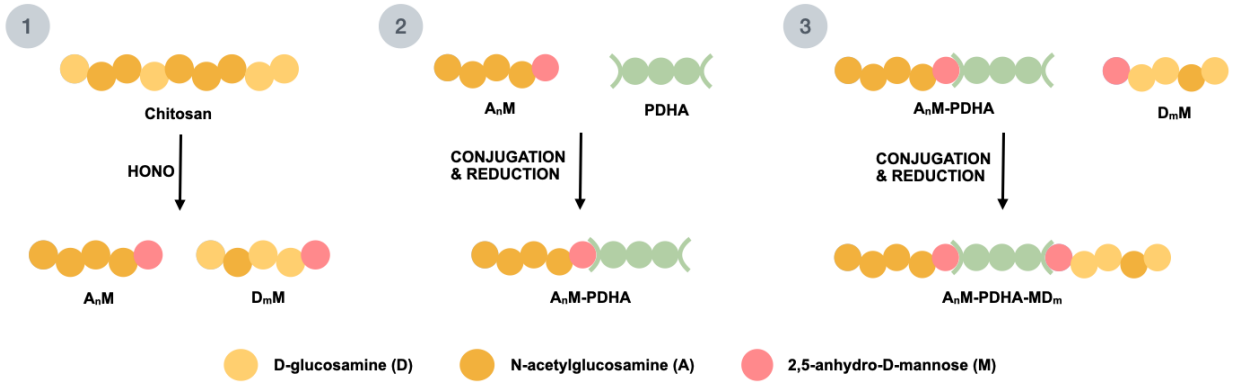

Figure 4.0.1: Overview of the preparation of chitin-*b*-chitosan diblocks.

4.1 Upscaling A_nM oligomers

4.1.1 Large-scale SEC fractionation

A_nM oligomers were prepared as previously described by Mo *et al.* [22], where chitosan (F_A = 0.48, 20 mg/mL) was degraded by nitrous acid (1.3 x D-units). For upscaling purposes, the degradation mixture was fractionated using a high-capacity SEC system (two Superdex 30 columns (BPG 140/950, GE Healthcare Bio-Science) in series). Figure 4.1.1a and 4.1.1b show SEC chromatograms of large-scale and small-scale fractionation, respectively. The latter figure is included for comparison, and was acquired from the PhD thesis of Ingrid V. Mo [21]. Both chromatograms show the same distinct separation pattern, although at different elution times. However, the elution rate is constant, making a comparison possible. Further, the separation near the salt peak in Figure 4.1.1a is more defined than in Figure 4.1.1b. ^{1}H-NMR characterization showed that the DP distribution of Figure 4.1.1a was in accordance with Figure 4.1.1b, indicating that the protocol is reproducible at a larger scale.

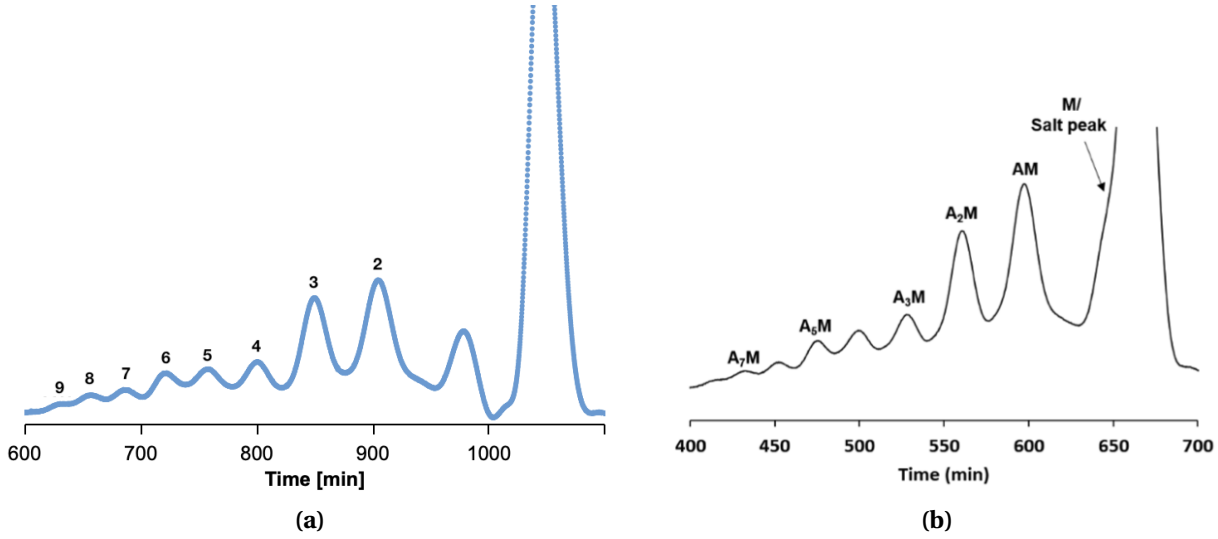

Figure 4.1.1: SEC chromatograms of A_nM oligomers using **(a)** large-scale fractionation (two Superdex 30 columns (BPG 140/950) in series) and **(b)** small-scale fractionation. Figure **(b)** is acquired from the PhD thesis of Ingrid V. Mo [21], and is included for comparison.

4.1.2 Desalting by centrifugal filtration

Centrifugal filtration was explored as a time-saving alternative to dialysis and evaporation when purifying large SEC fraction volumes. First, small-scale testing was done using two different membrane materials: regenerated cellulose and polyethersulfone (PES), where the MWCOs were 3 kDa. A selection of polymer samples (1 mg/mL) with known dialysis characteristics was tested, which comprised hyaluronic acid (HA, DP 10), β(1,3)-glucan (SBG, DP 10), alginate G-blocks (DP 7 and 20) and dextran (Dext, DP 34). To study the actual MWCO of the membrane materials, each sample was analyzed by HPAEC-PAD, where the chromatograms are shown in Figures A.1-A.5.

Unfortunately, chitin and chitosan are incompatible with HPAEC-PAD, thus the MWCO could not be analyzed directly for these polymers. For all the samples, there were no visible difference in the chromatograms between the retentate and the unfiltered sample, indicating that oligomers as short as dimers were withheld by the filters. Table 4.1.1 shows the membrane performances measured by their filtration rate from 10 mL to 0.5 mL. Here, regenerated cellulose was faster and more consistent than PES, hence the material of choice for large-scale filtration.

Table 4.1.1: Small-scale centrifugal filtration using regenerated cellulose and polyethersulfone (PES) membrane materials (MWCO = 3 kDa). The filtration rates of hyaluronic acid (HA, DP 10), β(1,3)-glucan (SBG, DP 10), alginate G-blocks (DP 7 and 20) and dextran (Dext, DP 34) (1 mg/mL, 4000 rcf, RT) for the membrane materials are presented.

Polymer	PES membrane filtration rate [mL/min]	Cellulose membrane filtration rate [mL/min]
HA	0.2	0.38
SBG	0.17	0.38
G_7	0.14	0.38
G_{20}	0.24	0.35
$Dext_{34}$	0.27	0.38

Based on the successful small-scale testing, large-scale centrifugal filtration was carried out using Centricon Plus-70 centrifugal filters (MWCO = 3 kDa), in which the purification yields are summarized in Table 4.1.2. Here, the purification method proved unsuccessful for A_2M, A_4M and A_9M, with yields ranging from only 1-11%. In comparison, purification of A_4M by freeze-drying resulted in a yield of 58%. Purification of SBG proved to be difficult, as the high concentration factor resulted in precipitation. Further, HPAEC-PAD analysis of the SBG filtrate, presented in Figure 4.1.2, showed visible amounts of oligomers with a DP < 10. This contradicts the findings for small-scale testing. However, centrifugal filtration was successful in purifying G_{19}-*b*-$Dext_{45}$ / $Dext_{45}$-PDHA, with a yield of 88%. The results for SBG and alginate were kindly provided by Celine E. Eidhammer and Victor Zylla Fæsther, respectively.

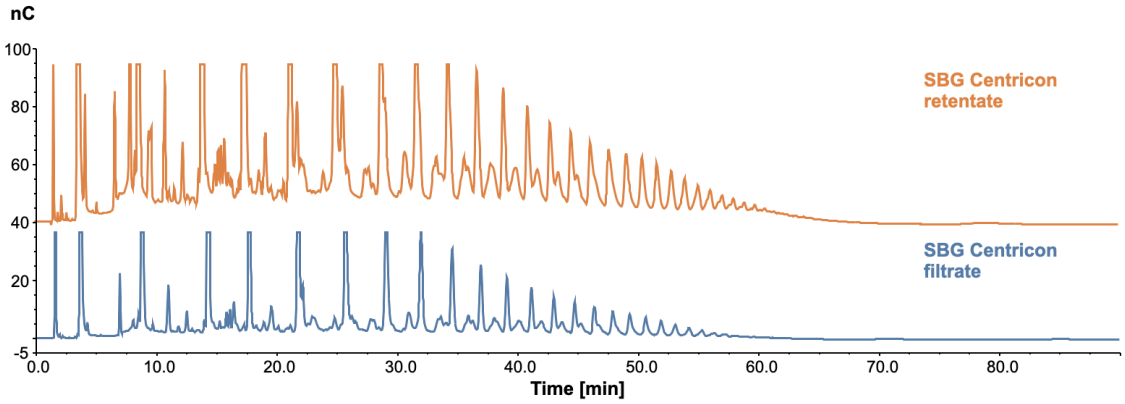

Figure 4.1.2: HPAEC-PAD chromatographs of the retentate and filtrate of purified acid hydrolyzed β(1,3)-glucan (SBG, DP 10, 1 mg/mL) using centrifugal filtration (Centricon Plus-70 centrifugal filters, MWCO = 3 kDa, Millipore). The results are kindly provided by Celine E. Eidhammer.

Table 4.1.2: Yields of $A_n M$ oligomers and a G_{19}-*b*-$Dext_{45}$ diblock purified by centrifugal filtration using Centricon Plus-70 centrifugal filters (MWCO = 3 kDa, Millipore). The diblock results were kindly provided by Victor Zylla Fæsther.

Polymer	DP	Yield [%]
$A_n M$	3	1
	5	6
	10	11
G_{19}-*b*-$Dext_{45}$ / $Dext_{45}$-PDHA	66	88

4.1.3 Characterization by ^{1}H-NMR

The DP of the oligomers from the SEC chromatogram in Figure 4.1.1a was confirmed by ^{1}H-NMR characterization, where Figure 4.1.3a and Figure 4.1.3b show ^{1}H-NMR spectra of A_4M purified by centrifugal filtration and freeze-drying, respectively. For both spectra, resonances for H1-A were observed at 4.45-4.52 ppm, while H1-M had a signal at 4.93 ppm. Minor resonances at 5.05 ppm were assigned to be alternative forms of the M residue, H1-M' [22]. As seen by the difference in peak size, there was some loss of M residue during the freeze-drying process. Moreover, an unidentified peak at 4.91 ppm was present in the spectrum for centrifugal filtration, thus assumed to be a contaminant.

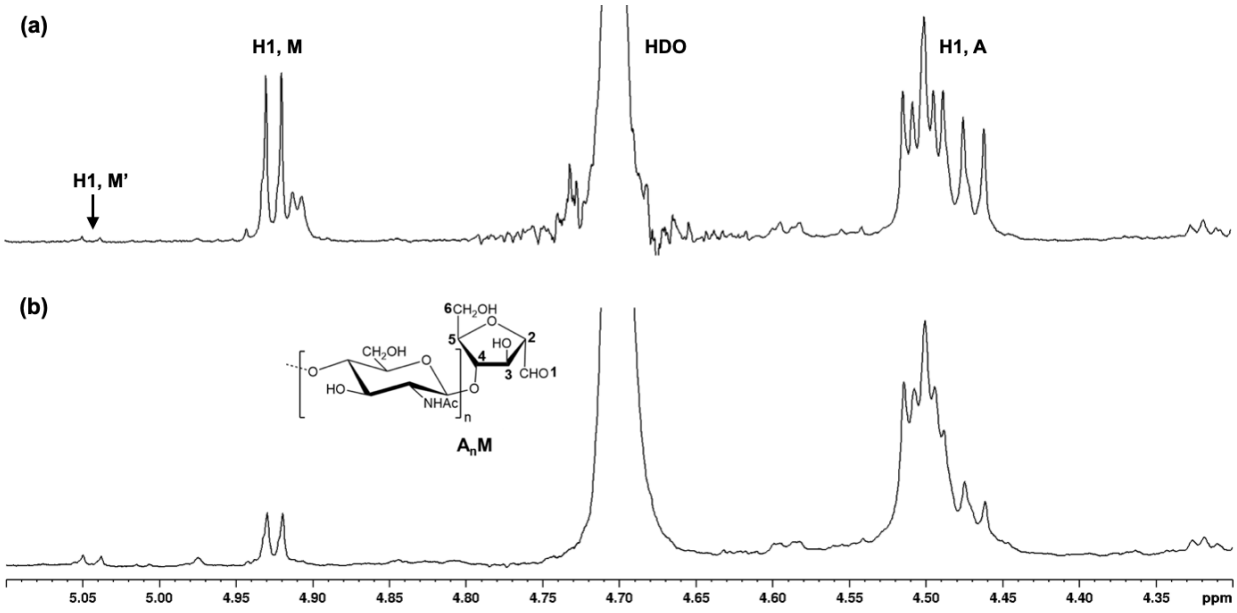

Figure 4.1.3: ^{1}H-NMR spectra (600MHz, RT, D_2O) of A_4M purified by **(a)** centrifugal filtration and **(b)** freeze-drying. The spectra are annotated according to literature [22,43], with the exception of M", which refers to an unidentified form of M.

4.2 D_nM oligomers

4.2.1 Preparation and fractionation

The protocol for D_nM oligomers developed by Gravdahl *et al.* [12] was reproduced. Here, D_nM oligomers obtained by HONO degradation (0.25 x D-units) of chitosan (F_A< 0.002, 20 mg/mL) were separated using small-scale SEC fractionation (0.1 M NaAc, pH 4.5), resulting in the chromatogram shown in Figure 4.2.1a. Figure 4.2.1b is a chromatogram acquired from the Master's thesis of Mina Gravdahl [12], and is included for comparison. Here, AmAc (0.15 M, pH 4.5) was used as the mobile phase for D_nM fractionation. The separation was almost identical for the two conditions, indicating that NaAc is a good alternative to AmAc. Due to the protocol and separation for D_nM oligomers being the same, the DP range was assumed to correspond with each other. The yields of purified D_nM oligomers of DP 3-15 are presented in Table 4.2.1, along with the estimated yields based on integration of the SEC chromatogram. Here, significant loss of recovery can be seen, with the majority of yields being < 10%. D_nM with DP 12-15 had yields of 13-24%.

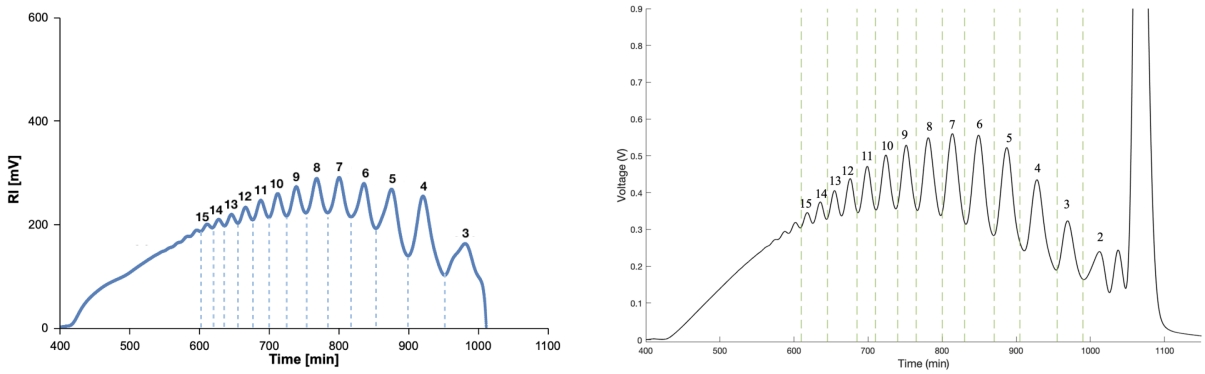

(a) **(b)**

Figure 4.2.1: SEC chromatograms of DnM oligomers using SEC-system 1 (three Superdex 30 columns in series (HiLoad 26/60)) eluting **(a)** NaAc buffer (0.1 M, pH 4.5, 0.8 mL/min) and **(b)** AmAc buffer (0.15 M, pH 4.5, 0.8 mL/min). Figure **(b)** is acquired from the Master's thesis of Mina Gravdahl [12] and is included for comparison.

Table 4.2.1: Yields of purified D_nM oligomers obtained by HONO degradation (0.25 x D-units) of chitosan (20 mg/mL, F_A < 0.002). The estimated mass is based on integration of the SEC chromatogram in Figure 4.2.1a.

DP	3	4	5	6	7	8	9	10	11	12	13	14	15
Total mass [mg]	1.2	1.2	1.6	3.0	3.5	2.4	1.9	3.1	2.1	3.9	4.5	5.3	2.5
Estimated mass [mg]	38	55	54	48	50	46	41	37	31	28	25	22	19
Yield [%]	3	2	3	6	7	5	5	8	7	14	18	24	13

4.2.2 Protocol discrepancies

Due to poor recovery of $D_n M$, a second batch was prepared following the protocol described in Section 3.6, but with a difference in how chitosan was dissolved. Here, AcOH (100 vol%) was added after chitosan to a final concentration of 2.5 vol%, instead of chitosan being dissolved in AcOH (2.5 vol%) directly. Figure C.1 illustrates the protocol for the batches, along with a control batch. Prior to degradation, batch 2 was visibly less viscous than batch 1 and the control batch, indicating a fundamental difference. The SEC chromatograms for batch 1, 2 and the control are presented in Figure C.2, where it can be seen that batch 2 is fully degraded compared to the others, which was unexpected.

4.2.3 Characterization by ^{1}H-NMR

The fraction corresponding to DP 6 in Figure 4.2.1a was further characterized by ^{1}H-NMR, and is shown in Figure 4.2.2. Resonance signal for H1-M is observed at 5.0 ppm, with minor resonances at 5.1 ppm arising from H1-M'. Self-branching by Schiff base reaction during the freeze-drying process is observed at 7.9 ppm. Further, loss of M-unit is seen by resonance signals at 5.3 and 4.9 ppm corresponding to H1-α and H1-β, respectively, at the reducing end of D. The H2-D internal residues can be observed at 2.72 ppm. An unknown signal at 4.5 ppm was also observed. Minor resonance signals at 4.3 and 4.1 ppm correspond to H3-M and H4-M, respectively. Notably, peaks at 3.57 and 3.47 ppm indicate the presence of glycerol, whereas signals at 1.24 and 4.1 ppm correspond to isopropanol. ^{1}H-NMR spectra of the contaminants are presented in greater detail in Figure B.1. The chemical shift of H5-M is overlapped by the CH resonance signal from isopropanol, as it would be observed at 4.0-4.1 ppm. Table 4.2.2 shows the yield of chitosan oligomers with M- or D-residue at the reducing end, as well as Schiff base conversion for D_5M and $D_{10}M$. The yields were obtained by peak integration of the ^{1}H-NMR spectra presented in Figure B.2.

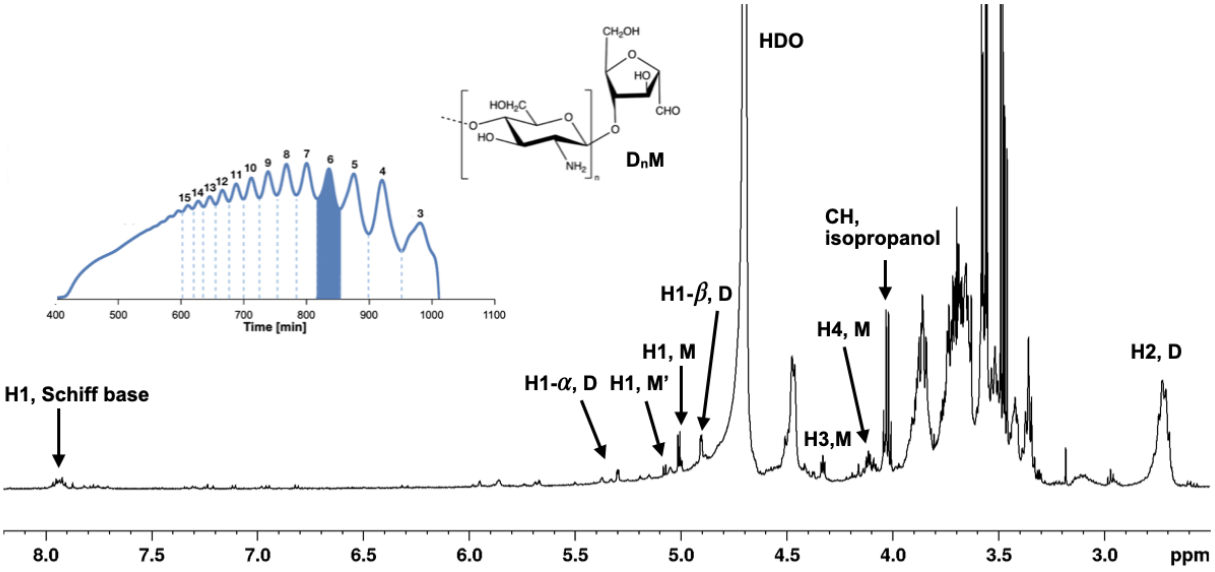

Figure 4.2.2: ^{1}H-NMR spectra (600MHz, RT, D_2O) of D_5M (fraction with assumed DP 6 in the chromatogram shown in Figure 4.2.1a). The spectrum is annotated according to literature [43].

Table 4.2.2: Yield of chitosan oligomers with M- or D-residue at the reducing end, and yield of Schiff bases. The yields were obtained by peak integration of ^{1}H-NMR spectra for D_5M and $D_{10}M$ shown in Figure B.2.

	M at the reducing end [%]	D at the reducing end [%]	Schiff base [%]
D_5M	49	12	39
$D_{10}M$	45	11	38

4.3 PDHA-activated A_nM oligomers

4.3.1 Preparation and fractionation

The second step in chitin-*b*-chitosan diblock preparation involved activating A_4M (20.5 mM) with PDHA (205 mM, 5 hours, RT) and reducing with PB (410 mM, 48 hours, 40°C), before subsequent purification and characterization. Three batches were prepared due to insufficient amounts of product, using A_4M purified by freeze-drying, and are summarized in Table 4.3.1. Batch 1 and 2 were dialyzed with a MWCO = 3.5 kDa, resulting in conjugate mixture yields of 2.9% and 1.5%, respectively. Based on these results, batch 3 was dialyzed using a MWCO = 500-1000 Da, resulting in a yield of 78.9%. Further, the A_4M-PDHA reaction mixture from batch 3 was fractionated by small-scale SEC fractionation (0.1 M NaAc, pH 4.5), in which the chromatogram is presented in Figure 4.3.1. Here, there are two main peaks consisting of a few smaller peaks. This is considerably different than previously reported in literature, and may indicate contaminants. The dotted lines indicate the fraction that was pooled for further ^{1}H-NMR characterization.

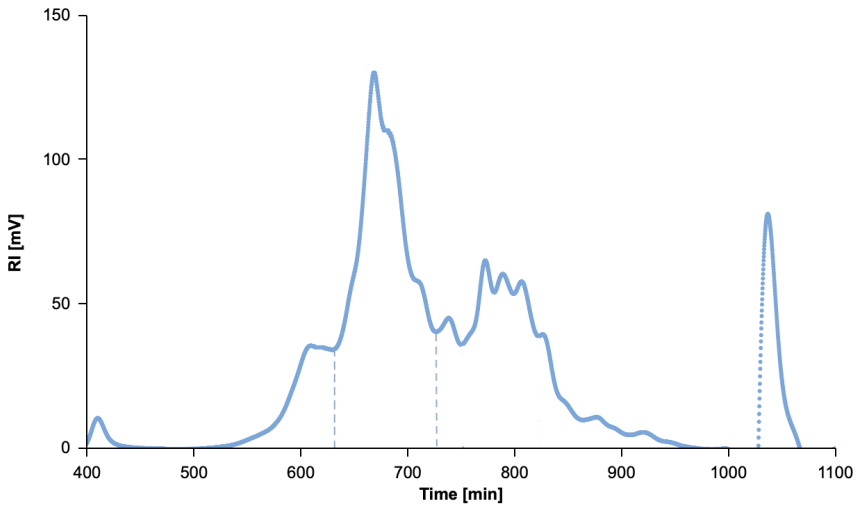

Figure 4.3.1: SEC chromatogram of A_4M-PDHA conjugates using SEC-system 1 eluting NaAc buffer (0.1 M, pH 4.5), where the dotted lines indicate the fraction that was further analyzed.

Table 4.3.1: Preparation of A_4M-PDHA conjugates by conjugating A_4M to PDHA, reducing with PB and purifying by dialysis. Yield corresponds to the A_4M-PDHA reaction mixture prior to fractionation.

Batch	A_4M [mM]	PDHA [mM]	PB [mM]	MWCO [Da]	Yield [%]
1	10.3	103	206	3500	2.9
2	20.5	205	410	3500	1.5
3	20.5	205	410	500-1000	78.5

4.3.2 Characterization by ^{1}H-NMR

Purified A_4M-PDHA was characterized by ^{1}H-NMR and compared to A_4M, as shown in Figure 4.3.2. Conjugation proved successful as seen by the resonance signals at 2.92 and 3.04 ppm confirming secondary amines. An unidentified peak can be seen at 1.83 ppm and is assumed to be a contaminant. The acetyl resonance signal overlap the CH_2 signal from PDHA, where it would be seen around 2.0 ppm as shown in Figure 2.3.2a. H1-A was observed at 4.45-5.52 ppm, and minor resonances at 4.93 ppm corresponding to H1-M, confirmed unreacted A_4M. This is likely due to cross-contamination from the smaller neighboring peak around 730 minutes.

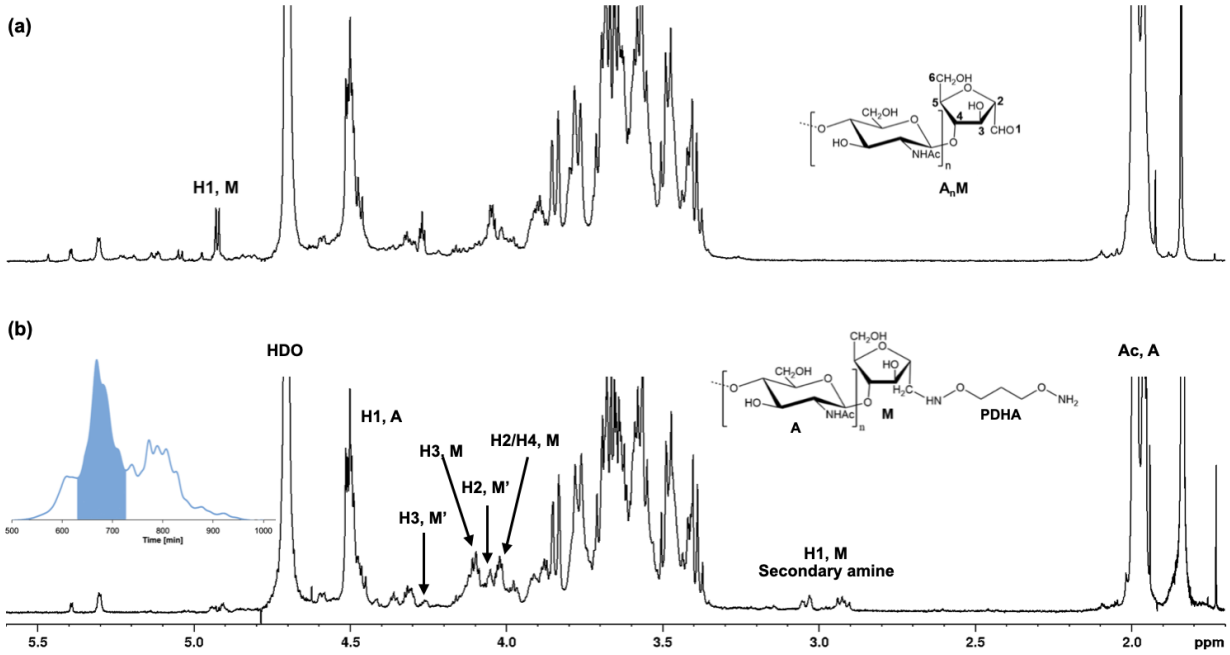

Figure 4.3.2: ^{1}H-NMR spectra (600MHz, RT, D_2O) of purified **(a)** A_4M and **(b)** A_4M-PDHA (the pooled fraction from Figure 4.3.1). The spectra are annotated according to literature [22].

4.4 A_4M-*b*-MD_5 diblocks

4.4.1 Preparation and fractionation

The final step in the preparation of a chitin-*b*-chitosan diblock comprised conjugating A_4M-PDHA and D_5M in equimolar ratios (8.0 mM) for 6 hours at RT. Due to insufficient amounts of D_nM oligomers, an in-house sample prepared by Jesper E. Pedersen (Department of Biotechnology, NTNU) was used. The subsequent reduction and purification was done as described for A_4M-PDHA, here with a MWCO = 3.5 kDa. Separation of reacted and unreacted products was done by small-scale SEC fractionation (AmAc, 0.15 M, pH 4.5), in which the resulting chromatogram is shown in Figure 4.4.1. Here, the three fractions of 1.0 mg were further characterized by ^{1}H-NMR. Due to the peaks being in close proximity to each other, cross-contamination is highly probable.

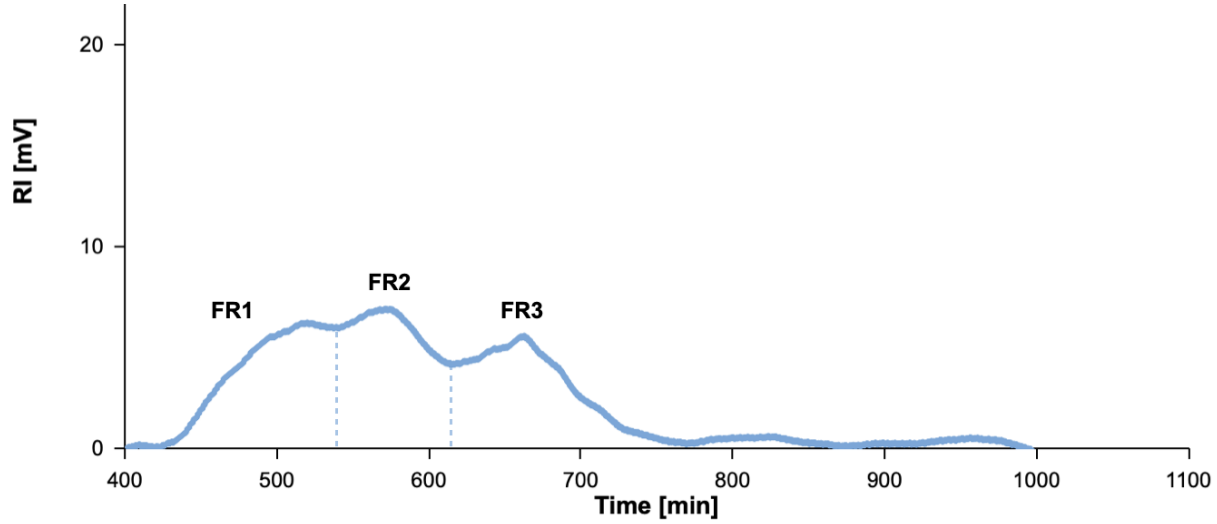

Figure 4.4.1: SEC chromatogram of the A_4M-PDHA-MD_5 diblock reaction mixture. Small-scale SEC fractionation was used, eluting AmAc buffer (0.15 M, pH 4.5).

4.4.2 Characterization by ^{1}H-NMR

The ^{1}H-NMR spectra of fraction 1-3 from the chromatogram in Figure 4.4.1 are presented in Figure 4.4.2. To identify the conjugates, both proton resonance signals and corresponding peak areas were used. A comparison of expected and actual peak area for the main resonance signals is shown in Table 4.4.1. H2-D internal residues were confirmed by a resonance signal at 2.67 ppm in all three spectra, and its peak area was set to 5.00 as a reference. In fraction 1 and 2, signals of H1-A was observed at 4.45-4.53 ppm, albeit somewhat obscured by an unknown peak at 4.42 ppm. Nevertheless, this unknown peak is included in the peak area for H1-A, as the area would otherwise be too small for a DP of 5. Secondary amines were confirmed by peaks at 2.84-3.0 ppm, thus the conjugation was successful. However, signals at 4.90 ppm confirmed the presence of H1-M in A_4M, so the conjugation was not complete. Moreover, the peak area for secondary amines was 2.06 and 1.34 for fraction 1 and 2, respectively, which is approximately half of the expected area. Due to the spectra of fraction 1 and 2 being almost identical, it is believed that both are diblocks, with fraction 2 being slightly shorter despite the larger combined peak area.

In fraction 3, the secondary amine resonance signals were more pronounced, as with H1-A, hence this is believed to be unreacted A_4M-PDHA, A_4M and D_5M. This is also in accordance with the elution time of A_4M-PDHA. The resonance signals for CH_2 in PDHA at 2.0 and 4.1 ppm is believed to be overlapped by the signals for acetyl and M, respectively. A comparison of D_5M, A_4M-PDHA and A_4M-PDHA-MD_5 is shown in Figure 4.4.3. The spectra show that the resonance signals for H2-D and secondary amines are slightly shifted, which may be due to changes in pH.

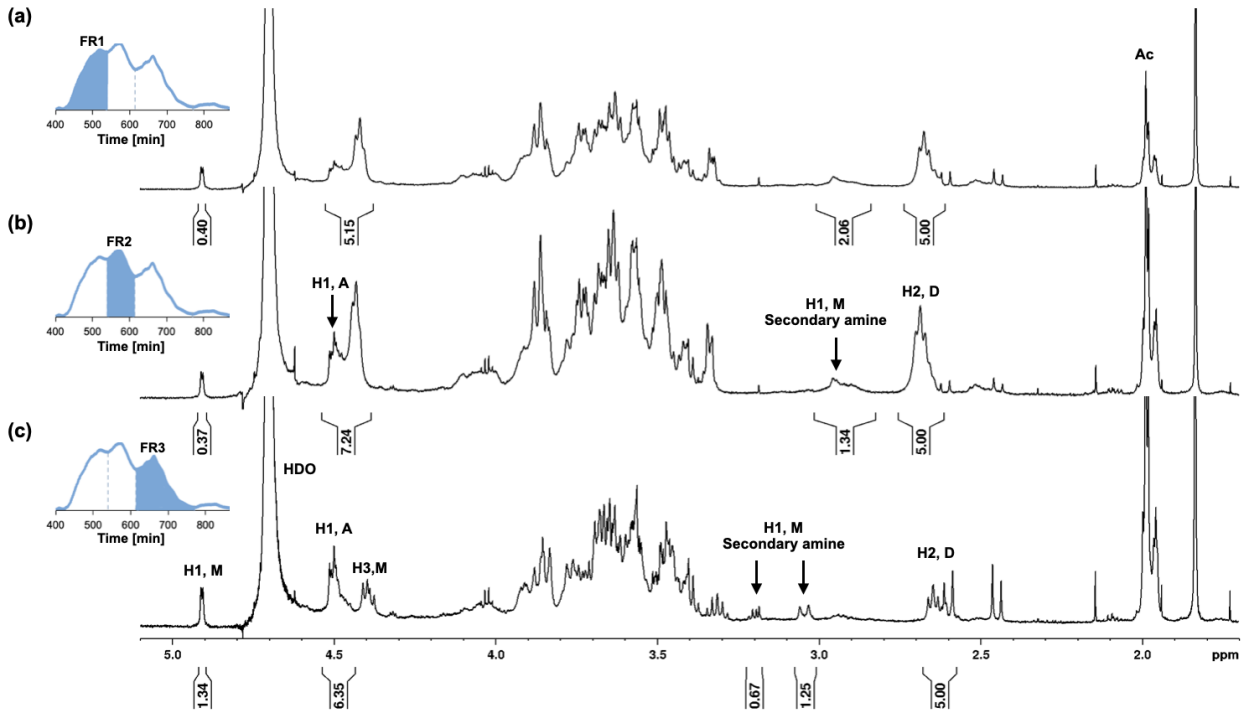

Figure 4.4.2: ^{1}H-NMR spectra (600MHz, RT, D_2O) of **(a)** fraction 1, **(b)** fraction 2 and **(c)** fraction 3 from the SEC chromatogram in Figure 4.4.1. The spectrum is annotated according to literature [21,12].

Table 4.4.1: Expected and actual peak area for the annotated resonance signals in Figure 4.4.2 of the A_4M-*b*-MD_5 reaction mixture. *H2,D was set to 5.00 as the integral reference.

Fraction	Resonance signal	Expected peak area	Actual peak area
1	H1, A	4	5.15
	H2, D	5	5.00*
	H1, M	0	0.40
	H1, M secondary amines	4	2.06
2	H1, A	< 4	7.24
	H2, D	5	5.00*
	H1, M	0	0.37
	H1, M secondary amines	4	1.34
3	H1, A	4	6.35
	H2, D	5	5.00*
	H1, M	0	1.34
	H1, M secondary amines	1 + 1	0.67 + 1.25

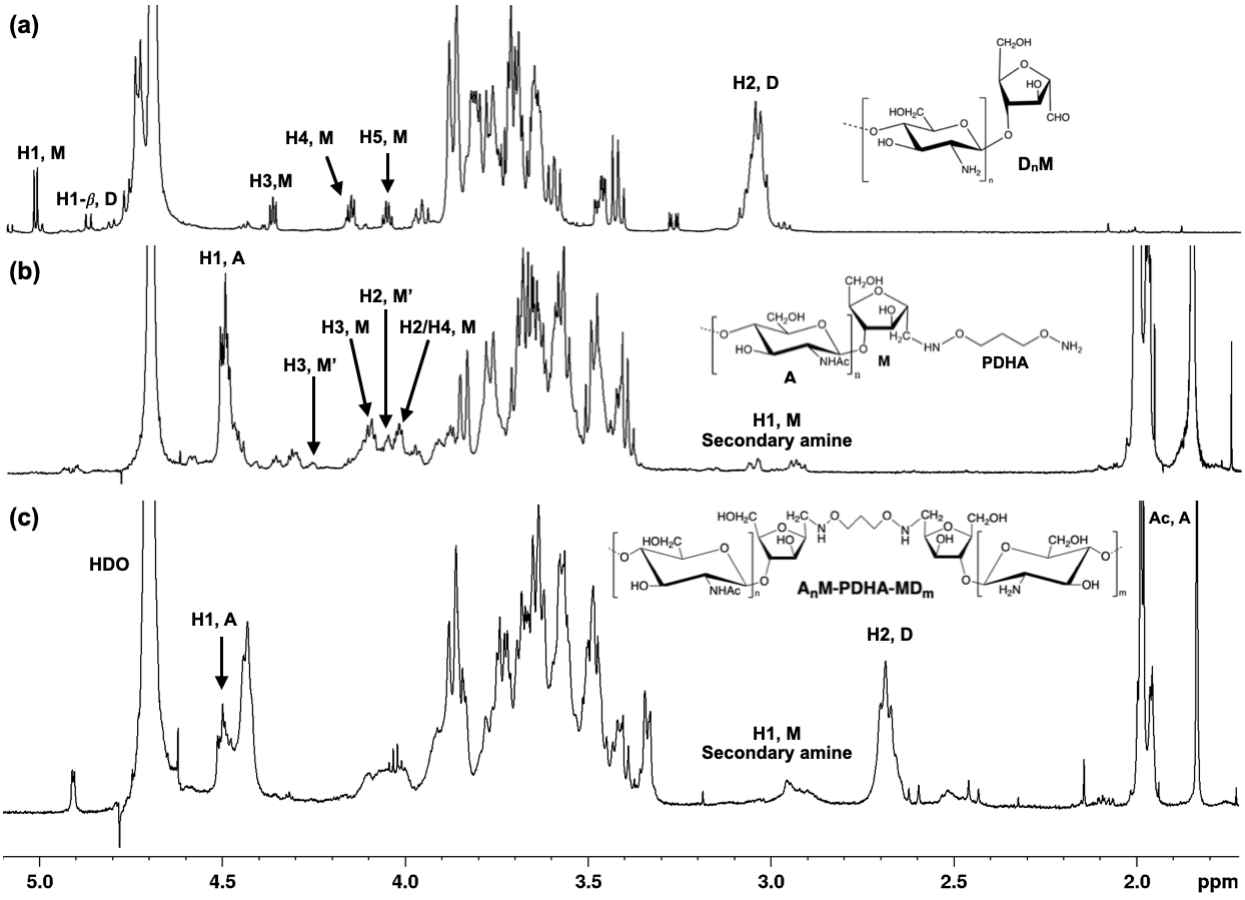

Figure 4.4.3: ^{1}H-NMR spectra (600MHz, RT, D_2O) of purified **(a)** D_5M, **(b)** A_4M-PDHA and **(c)** A_4M-*b*-MD_5 (fraction 1 in the SEC chromatogram in Figure 4.4.1). The spectra are annotated according to literature [21,12].

5 | Discussion

To reiterate the scope of this thesis, Figure 1.2.1 is presented once more. The key aspects were to explore a method for upscaling oligomers, specifically A_nM, and prepare and characterize chitin-*b*-chitosan diblocks. This also included developing a protocol for said diblock preparation.

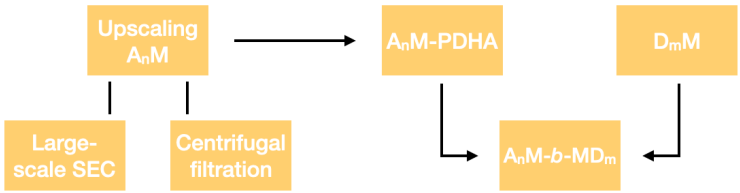

5.1 Upscaling A_nM oligomers

A common concern when using broad SEC fractionation is poor separation. However, A_nM preparation using large-scale SEC fractionation proved to be successful when compared to previous results of a study by Mo *et al.* [21]. As seen in Figure 4.1.1, the SEC separations are almost identical, and subsequent ^{1}H-NMR characterization confirmed the DP range to be in accordance with the study. The resolution of the separation is accurate enough to pool fractions of DP 10, albeit being close to the neighboring peak. To remove any cross-contamination in a fraction, narrow fractionation can be used. These results show the reproducibility of A_nM preparation, in addition to its ability to be upscaled.

When upscaling oligomer preparation, the volume of pooled SEC fractions increase significantly (from < 1 L to > 10 L). Thus, current purification methods like evaporation and dialysis become tedious and time-consuming. Centrifugal filtration is commonly used in protein recovery to purify and concentrate solutions, and there is a variety of filtration devices on the market. Larger ones can concentrate and desalt solutions of 70 mL to 0.320 mL in 40 minutes [35], making this method very attractive for purification of large SEC fractions. To determine if this approach would be fruitful, small-scale testing on HA, SBG, alginate (G_7 and G_{20}) and $Dext_{34}$ was done using two different membrane materials; regenerated cellulose and PES (MWCO = 3 kDa). Here, the regenerated cellulose membrane had a constant filtration rate of 0.38 mL/min compared to PES, which varied between 0.14 to 0.27 mL/min.

Thus, regenerated cellulose was the membrane material of choice for further work. HPAEC-PAD analyses of unfiltered and filtered polymer solutions (HA, SBG, G_7, G_{20} and $Dext_{34}$) indicated that oligomers as short as dimers remained in the retentate, as there was no difference between the two chromatograms. However, during large-scale purification of A_nM and SBG oligomers using Centricon Plus-70 filters (MWCO = 3 kDa), the small-scale results were contradicted. The purification of A_2M, A_4M and A_9M only yielded 1, 6 and 11%, respectively. Since there was no visible precipitation or weight difference in the centrifugal filters, it is assumed that A_nM did not remain in the chambers. Further HPAEC-PAD analyses of purified SBG showed that chromatograms of the retentate and filtrate were almost identical, thus the filtrate contained oligomers with DP < 10. Due to chitin being inapplicable to HPAEC-PAD analysis, the SBG results were assumed to be valid for A_nM as well. These findings may have been observed earlier, had the filtrate of each sample from the small-scale testing been analyzed in addition to the retentate.

Nevertheless, centrifugal filtration proved successful in purifying G_{19}-*b*-$Dext_{45}$ diblocks, with a yield of 88%. This is in accordance with the Centricon Plus-70 data from Millipore, where a typical concentrate recovery was 87% using cytochrome c (0.25 mg/mL, MWCO = 3 kDa) as a marker. The main differences between these three polymers were their DP and charge. A_nM and SBG are both neutral polymers, whereas alginate is a polyanion. Whether or not the negative charge is a contributing factor in the filtration process, remains to be investigated. Based on the evident yield difference between A_nM and alginate, as well as the SBG filtrate result, it is believed that the majority of oligomers with a DP < 10 pass through the membrane, whereas oligomers with a DP > 10 remains in the retentate.

5.2 Preparation and characterization of D_nM oligomers

A protocol for preparation of D_nM oligomers with a high yield of M residue at the reducing end has been reported by Gravdahl [12], in which they obtained 84% and 87% of purified D_4M and D_9M, respectively. This was significantly higher than previous protocols, with yields of 50-70% [12]. Thus, when preparing D_nM oligomers in this thesis, their protocol was followed. However, NaAc buffer (0.1 M, pH 4.5) was explored as a new SEC mobile phase instead of AmAc (0.15 M, pH 4.5), due to ammonium increasing the pH to 8 during freeze-drying, resulting in self-branching by Schiff base reaction. SEC chromatograms of D_nM degradation mixtures using NaAc -and AmAc buffers (Figures 4.2.1a and 4.2.1b, respectively) were almost identical, indicating that the new buffer is a good alternative to AmAc. However, ^{1}H-NMR of D_5M and $D_{10}M$ confirmed self-branching of 39 and 38%, respectively, despite the change in buffer and use of dialysis prior to freeze-drying. This indicates that self-branching can occur at pH < pK_a which is lower than previously assumed. These mechanisms are complicated and susceptible to changes which are yet to be understood, and should be further investigated. Moreover, the yield of M at the reducing end was 49 and 45% for D_5M and $D_{10}M$, which is significantly lower than previously reported.

Despite being purified by dialysis, the ^{1}H-NMR spectrum of D_5M showed the sample was contaminated by glycerol and isopropanol (Figure B.1). Cross-contamination during freeze-drying has been known to happen, however, not to this extent. To our knowledge, isopropanol was not used by anyone while freeze-drying D_nM. As for glycerol, dialysis bags have a glycerol coating on the inside which may be the source of contamination. Nevertheless, glycerol is a small molecule expected to be removed during dialysis. Further, no isopropanol or glycerol contamination was observed for A_4M or A_4M-PDHA, indicating it was a single occurrence.

As summarized in Table 4.2.1, significant loss of material was observed after the purification process. The majority of the loss concerns D_nM oligomers of DP 3-11, with yields < 10%. As the degradation mixture was freeze-dried prior to fractionation, the amount separated by SEC is known. Thus, the only obvious steps where loss could occur would be during dialysis and / or inside the SEC columns. This is further discussed in Section 5.5, as low recovery was a recurring observation throughout the diblock preparation. Due to the low recovery, a second batch was prepared using the same protocol except that AcOH (100 vol%) was added after chitosan to a final concentration of 2.5 vol% (Figure C.1). This chitosan solution was visibly less viscous than the first batch prior to HONO degradation, so a control batch was prepared as batch 1. Comparing SEC chromatograms of batch 1, 2 and the control batch, batch 2 was fully degraded. This may be due to a localized degradation caused by the concentrated AcOH upon adding it to the chitosan solution, even though the final concentration was dilute. A study by Vårum *et al.*[48] showed that the rate constants for cleaving of D-A and D-D are negligible compared to those of A-A and A-D, thus A-D govern the degradation. If the degradation rate constant for A-D, k_{A-D}, is used to obtain the theoretical degradation in batch 2, the effects of concentrated AcOH can be determined (Section C.2). Nevertheless, as shown in Figure C.3, the change in DP under the said conditions was < 1% after 3 minutes, thus having a negligible effect. Hence the cause for decreased viscosity and increased degradation is presently unknown.

5.3 Preparation and characterization of A_nM-PDHA

In the preparation of A_4M-PDHA, three batches were made due to insufficient product. Batch 1 and 2 were dialyzed with a MWCO = 3.5 kDa, whereas batch 3 used a MWCO = 500-1000 Da. This resulted in reaction mixture yields of 2.9, 1.5 and 78.5%, respectively (Table 4.3.1). The difference in yields is considerably high, indicating that a MWCO = 3.5 kDa is inappropriate for oligomers with a DP < 10. Batch 3 was further fractionated in which the chromatogram displayed two main peaks that were notably split into a few minor peaks. This is not in accordance with literature. The smaller peak around 730 minutes may correspond to unreacted A_4M, whereas unreacted PDHA and PB may correspond to the later peaks. Nevertheless, the increase in number of peaks is without further analysis assumed to be contaminants. ^{1}H-NMR characterization confirmed a successful conjugation, however, unreacted A_4M was present and is likely due to cross-contamination. An unidentified singlet around 1.8 ppm is present in both A_4M and A_4M-PDHA, and the acetyl signal at 2.0 is believed to hide the multiplet of CH_2 in PDHA (Figure B.4). Similarly, the resonance signals for the M residue overlap with the signal corresponding to the triplet of CH_2 in PDHA.

5.4 Preparation and characterization of A_4M-*b*-MD_5 diblock

For the conjugation of D_5M to A_4M-PDHA, an in-house sample prepared by Jesper E. Pedersen (Department of Biotechnology, NTNU) was used due to insufficient amounts of D_nM oligomers. The reaction mixture was separated into three fractions of 1.0 mg, and characterized by ^{1}H-NMR. Fraction 1 and 2 both appeared to be diblocks, indicating that the diblock yield is approximately 30-60%. Fraction 3 is believed to be unreacted A_4M-PDHA and D_5M, as well as free A_4M. The main difference between fraction 1 and 2 was a slight increase and decrease in peak area of H1-A and secondary amines, respectively. This may be explained by the presence of free A_4M that has been cleaved off, as confirmed by H1-M resonance signals. However, the H1-M peak area is approximately 0.4 in both spectra, thus the differences may be caused by other factors. The unknown resonance signal at 4.42 ppm is not present in the ^{1}H-NMR spectra of D_5M and A_4M-PDHA used in the conjugation, however a similar peak can be seen in the spectrum of D_5M prepared in this thesis. Further, the resonance signal for unreacted D_5M in fraction 3 differ in shape and is more distinct, compared to the corresponding signal in fraction 1 and 2, and Figure B.3. Nevertheless, without further investigation, nothing certain can be said. Relative to the H2-D peak area, the increase of the H1-A peak area in all three spectra may be due to cross-contamination of A_4M as the fractions are in high proximity to each other. Based on the peak areas of H1-A, secondary amines and H2-D, fraction 1 is believed to be A_4M-PDHA-MD_5. Despite eluting later in the SEC chromatogram, fraction 2 show a slightly higher DP than fraction 1, which is inconsistent with the principles of SEC. A higher DP than the starting materials is not possible, hence fraction 2 is believed to be a shorter diblock than fraction 1.

5.5 Possible factors resulting in low recovery

A recurring observation throughout the preparation of the chitin-*b*-chitosan diblock was low recovery. Material loss to this extent has not been previously reported when working with A_nM- and D_nM oligomers, thus it was surprising. The two main sources of loss are believed to be inside the SEC columns and during dialysis. It is important to note that MWCO is a term originally used when describing proteins, which are mostly globular and compact, contrary to flexible polysaccharides with extendable chains. Hence, globular proteins may only be a few nanometers in diameter despite having a large molecular weight. Due to oligomers typically being larger than proteins, a MWCO exceeding the molecular weight of the oligomer may still be used. However, there are various factors that can interfere, making MWCO a guide rather than a rule. Based on the centrifugal filtration results of A_nM and SBG, as well as the dialysis of A_4M-PDHA, it is clear that a MWCO = 3-3.5 kDa is inappropriate for DP < 10. Further, material loss inside the SEC columns may be seen in the purification of A_4M oligomers by freeze-drying, where the yield was only 58%. For the recovery of D_nM oligomers, the yields were < 10% for DP 3-11. However, these fractions were dialyzed prior to freeze-drying, so the culpable step is ambiguous. Nevertheless, chitosan is a polycation that can interact with the negatively charged stationary phase, and remain inside the column.

6 | Conclusion and further work

This thesis has provided preliminary insight into the preparation and characterization of chitin-*b*-chitosan diblocks by conjugating A_4M-PDHA to D_5M. Moreover, the reproducibility of the protocols for A_nM- and D_nM oligomers by Mo *et al.* and Gravdahl *et al.*, has been explored. Upscaling of A_nM oligomers proved to be successful when comparing chromatograms of large-scale and small-scale SEC fractionation, thus providing an efficient method for separation of samples > 200 mg. Centrifugal filtration (MWCO = 3 kDa) was explored as a time-efficient alternative to dialysis and evaporation, and small-scale testing on HA, SBG, alginate G-blocks and dextran showed that dimers were withheld by the filter. However, large-scale purification proved unsuccessful with yields ranging from 1-11% for oligomers with a DP < 10. Nevertheless, it was highly successful for a G_{19}-*b*-$Dext_{45}$ diblock, with a yield of 88%.

Throughout the preparation of D_nM and A_nM-PDHA, significant loss of material was observed which has not been previously reported. It is therefore assumed that a MWCO = 3.5 kDa during dialysis was inappropriate for oligomers with a DP < 10, and the majority of the loss may have occurred here. For A_nM-PDHA, a MWCO = 500-1000 Da resulted in a yield of 78.5%, which is significantly higher than the yield of < 3% for a MWCO = 3.5 kDa. However, in the preparation of D_nM oligomers, material could be lost inside the columns due to electrostatic interactions between chitosan (positively charged) and the stationary phase (negatively charged). The conjugation of A_4M-PDHA and D_5M was proved successful by ^{1}H-NMR characterization, with a yield of approximately 30% based on the SEC chromatogram.

The future of chitin-*b*-chitosan diblocks encompass mRNA / siRNA complexation for use in vaccines and gene therapy, respectively. Further research and optimization of the protocol is therefore needed. This may include exploring different purification techniques, such as precipitation, in which the conditions favor precipitation of unreacted oligomers. However, the solution properties of chitin-*b*-chitosan diblocks and D_nM-PDHA are yet to be studied, and remain of high interest. If successful, SEC may then only be used to obtain specific DPs, rather than separating reaction mixtures, resulting in a more time-efficient protocol. Moreover, diblocks with a longer chitosan block (DP > 10) is also of interest with respect to biomedical applications. Lastly, possible self-assembling properties of chitin-*b*-chitosan should be explored, by eg. dynamic light scattering.

Bibliography

[1] *Advanced Biopolymers AS* (2022). Available at: http://www.advancedbiopolymers.no (Accessed: 23/03/22).

[2] Alexandridis, P. and Lindman, B. (2000). *Amphiphilic block copolymers: Self-assembly and applications*, 1 edn, Elsevier.

[3] Allan, G. and Peyron, M. (1995). Molecular weight manipulation of chitosan i: Kinetics of depolymerization by nitrous acid, *Carbohydrate Research* **277**(2): 273–282. doi: 10.1016/0008-6215(95)00207-a.

[4] Anitha, A. et al. (2014). Chitin and chitosan in selected biomedical applications, *Progress in Polymer Science* **39**(9): 1644–1667. doi: 10.1016/j.progpolymsci.2014.02.008.

[5] Bernkop-Schnürch, A. and Dünnhaupt, S. (2012). Chitosan-based drug delivery systems, *European Journal of Pharmaceutics and Biopharmaceutics* **81**(3): 463–469. doi: 10.1016/j.ejpb.2012.04.007.

[6] Cosenza, V. A., Navarro, D. A. and Stortz, C. A. (2011). Usage of α-picoline borane for the reductive amination of carbohydrates, *Arkat* **7**: 182–194. doi: 10.3998/ark.5550190.0012.716.

[7] Database, H. M. (2022a). *1H NMR Spectrum (1D, 500 MHz, H2O, experimental) (HMDB0000131)*, Available at: https://hmdb.ca/spectra/nmr_one_d/1101 (Accessed: 29/4/22).

[8] Database, H. M. (2022b). *1H NMR Spectrum (1D, 500 MHz, H2O, experimental) (HMDB0000863)*, Available at: https://hmdb.ca/spectra/nmr_one_d/1573 (Accessed: 29/4/22).

[9] Defaye, J. (1970). 2,5-anhydrides of sugars and related compounds, *Advances in Carbohydrate Chemistry and Biochemistry* **25**: 181–228. doi: 10.1016/S0065-2318(08)60428-X.

[10] Dionex (1998). Optimal settings for pulsed amperometric detection of carbohydrates using the dionex ed40 electrochemical detector, *Technical report*, Dionex Corporation.

[11] Draget, K. I. and Taylor, C. (2011). Chemical, physical and biological properties of alginates and their biomedical implications, *Food Hydrocolloids* **25**(2): 251–256. doi: 10.1016/j.foodhyd.2009.10.007.

[12] Gravdahl, M. (2020). *Preparation, characterization, and solution properties of chitosan-b-dextran diblocks*, Master's thesis, Norwegian University of Science and Technology.

[13] Hojo, K. et al. (2000). Facile synthesis of a chitosan hybrid of a laminin-related peptide and its antimetastatic effect in mice, *The Journal of Pharmacy and Pharmacology* **52**: 67–73. doi: 10.1211/0022357001773526.

[14] Holmås, E. (2021). *Preparation and characterization of PDHA-activated hyaluronic acid and chitin-b-dextran diblock structures*. Specialization project, Norwegian University of Science and Technology.

[15] Kostanski, L. K., Keller, D. M. and Hamielec, A. E. (2004). Size-exclusion chromatography—a review of calibration methodologies, *Journal of Biochemical and Biophysical Methods* **58**(2): 159–186. doi: 10.1016/j.jbbm.2003.10.001.

[16] Lee, C. G. et al. (2008). Chitin regulation of immune responses: an old molecule with new roles, *Current Opinion in Immunology* **20**(6): 684–689. doi: 10.1016/j.coi.2008.10.002.

[17] Liu, C. C., Chang, K. Y. and Wang, Y. J. (2010). A novel biodegradable amphiphilic diblock copolymers based on poly(lactic acid) and hyaluronic acid as biomaterials for drug delivery, *Journal of Polymer Research* **17**: 459–469. doi: 10.1007/s10965-009-9332-5.

[18] Mathur, N. K. and Narang, C. K. (1990). Chitin and chitosan, versatile polysaccharides from marine animals, *Journal of Chemical Education* **67**(11): 938. doi: 10.1021/ed067p938.

[19] Mechelke, M. et al. (2017). Hpaec-pad for oligosaccharide analysis—novel insights into analyte sensitivity and response stability, *Analytical and Bioanalytical Chemistry* **409**: 7169–7181. doi: 10.1007/s00216-017-0678-y.

[20] Mi, F. et al. (2001). Fabrication and characterization of a sponge-like asymmetric chitosan membrane as a wound dressing, *Biomaterials* **22**(2): 165–173. doi: 10.1016/S0142-9612(00)00167-8.

[21] Mo, I. V. (2021). *Towards block polysaccharides: Terminal activation of chitin and chitosan oligosaccharides by dioxyamines and dihydrazides and the preparation of block structures*, PhD thesis, Norwegian University of Science and Technology.

[22] Mo, I. V. et al. (2020a). 2,5-anhydro-d-mannose end-functionalized chitin oligomers activated by dioxyamines or dihydrazides as precursors of diblock oligosaccharides, *Biomacromolecules* **21**(7): 2884–2895. doi: 10.1021/acs.biomac.0c00620.

[23] Mo, I. V. et al. (2020b). Activation of enzymatically produced chitooligosaccharides by dioxyamines and dihydrazides, *Carbohydrate Polymers* **232**: 115748. doi: 10.1016/j.carbpol.2019.115748.

[24] Mori, S. and Barth, H. G. (1999). *Size Exclusion Chromatography*, Springer-Verlag, chapter 1.2: Brief Description of Size Exclusion Chromatography, pp. 4–5. doi: 10.1007/978-3-662-03910-6.

[25] Neves, N. M. et al. (2008). *Natural-Based Polymers for Biomedical Applications*, Woodhead. ISBN: 9781845694814.

[26] Noshay, A. and McGrath, J. E. (1977). *Block Copolymers: Overview and Critical Survey*, Academic Press, chapter 2: Polymer Hybrids, pp. 17–20. isbn: 0-12-521750-1.

[27] Novoa-Carballal, R. and Müller, A. H. E. (2012). Synthesis of polysaccharide-*b*-peg block copolymers by oxime click, *The Royal Society of Chemistry* **48**: 3781–3783. doi: 10.1039/C2CC30726J.

[28] Prabaharan, M. and Mano, J. F. (2004). Chitosan-based particles as controlled drug delivery systems, *Drug Delivery* **12**(1): 41–57. doi: 10.1080/10717540590889781.

[29] Rinaudo, M. (2006). Chitin and chitosan: Properties and applications, *Progress in Polymer Science* **31**(7): 603–632. doi: 10.1016/j.progpolymsci.2006.06.001.

[30] Rinaudo, M. (2007). Main properties and current applications of some polysaccharides as biomaterials, *Polymer International* **57**(3): 397–430. doi: 10.1002/pi.2378.

[31] Rohrer, J. (2013). Analysis of carbohydrates by high-performance anion-exchange chromatography with pused amperometric detection (hpae-pad), *Technical report*, Thermo Fisher Scientific. Available at: www.thermoscientific.com/dionex (Accessed: 30/4/22).

[32] Rohrer, J. S. and Bhattacharyya, L. (2012). *Applications of Ion Chromatography for Pharmaceutical and Biological Products*, Wiley & Sons, chapter 1: Ion Chromatography- Principles and Applications, pp. 18–26. isbn: 978-0-470-46709-1.

[33] Schatz, C. and Delas, T. (2021). Fundamental and practical aspects in the formulation of colloidal polyelectrolyte complexes of chitosan and sirna, *in* H. J. Ditzel et al. (eds), *Design and Delivery of siRNA Therapeutics. Methods in Molecular Biology*, Vol. 2282, Humana, pp. 297–327. doi: 10.1007/978-1-0716-1298-9_17.

[34] Shafizadeh, F. (1958). Formation and cleavage of the oxygen ring in sugars, *Advances in Carbohydrate Chemistry and Biochemistry* **13**: 9–61. doi: 10.1016/S0096-5332(08)60351-3.

[35] Sigma Aldrich (2021). User guide: Centricon® plus-70 centrifugal filter, *Technical report*, Millipore. Available at: https://www.sigmaaldrich.com/deepweb/assets/sigmaaldrich/product/documents/361/914/pr03221w-rev-0621-mk.pdf (Accessed: 28/5/22).

[36] Silverstein, R. M., Webster, F. X. and Kiemle, D. J. (2005). *Spectrometric Identification of Organic Compounds*, Wiley & Sons, chapter 3: Proton Magnetic Resonance Spectroscopy, pp. 127–129 and 137. isbn: 0-471-39362-2.

[37] Solberg, A. (2022). *Self-assembling alginate-based diblock polymers*, PhD thesis, Norwegian University of Science and Technology.

[38] Solomons, T., Fryhle, C. B. and Snyder, S. A. (2014). *Organic Chemistry*, Wiley, Singapore. ISBN: 978-1-118-65305-0.

[39] Strand, S. et al. (2001). Electrophoretic light scattering studies of chitosans with different degrees of n-acetylation, *Biomacromolecules* **2**(4): 1310–1314. doi: 10.1021/bm015598x.

[40] Sugiyama, H. et al. (2001). The conformational study of chitin and chitosan oligomers

in solution, *Bioorganic & Medicinal Chemistry* **9**: 211–216. doi: 10.1016/S0968-0896(00)00236-4.

[41] Thermo Fischer Scientific (2022). *NMR Proton Shifts for Residual Solvent Impurities*, Available at: https://beta-static.fishersci.com/content/dam/fishersci/en_US/documents/programs/scientific/brochures-and-catalogs/posters/nmr-proton-shifts-for-residual-solvent-impurities-poster.pdf (Accessed: 29/4/22).

[42] Tiwari, A. K. (2004). Antioxidants: new generation therapeutic base for treatment of polygenic disorders, *Current Science* **86**(8): 1092–1102. https://www.jstor.org/stable/24109318.

[43] Tømmeraas, K. et al. (2001). Preparation and characterisation of oligosaccharides produced by nitrous acid depolymerisation of chitosans, *Carbohydrate Research* **333**(2): 137–144. doi: 10.1016/S0008-6215(01)00130-6.

[44] Vandevord, P. J. et al. (2002). Evaluation of the biocompatibility of a chitosan scaffold in mice, *Journal of Biomedical Materials Research* **59**(3): 585–590. doi: 10.1002/jbm.1270.

[45] Volokhova, A. (2020). Polysaccharide-containing block copolymers: synthesis and applications, *Materials Chemistry Frontiers* **4**(1): 99–112. doi: 10.1039/C9QM00481E.

[46] Vårum, K. et al. (1991). Determination of the degree of n-acetylation and the distribution of n-acetyl groups in partially n-deacetylated chitins (chitosans) by high-field n.m.r. spectroscopy, *Carbohydrate Research* **211**(1): 17–23. doi: 10.1016/0008-6215(91)84142-2.

[47] Vårum, K. et al. (1994). Water-solubility of partially n-acetylated chitosans as a function of ph: Effect of chemical composition and depolymerisation, *Carbohydrate Research* **25**(2): 65–70. doi: 10.1016/0144-8617(94)90140-6.

[48] Vårum, K. et al. (2001). Acid hydrolysis of chitosans, *Carbohydrate Polymers* **46**(1): 89–98. doi: 10.1016/S0144-8617(00)00288-5.

[49] Williams, J. M. (1975). Deamination of carbohydrate amines and related compounds, *Advances in Carbohydrate Chemistry and Biochemistry* **31**: 9–79. doi: 10.1016/S0065-2318(08)60294-2.

[50] Yang, D. et al. (2020). Progress, opportunity, and perspective on exosome isolation - efforts for efficient exosome-based theranostics, *Theranostics* **10**: 3684–3707. doi: 10.7150/thno.41580.

[51] Yao, H.-Y.-Y. et al. (2021). A review of nmr analysis in polysaccharide structure and conformation: Progress, challenge and perspective, *Food Research International* **143**: 110290. doi: 10.1016/j.foodres.2021.110290.

Appendices

A HPAEC-PAD chromatograms

Figures A.1-A.5 show HPAEC-PAD chromatograms of purified and unpurified samples of HA, SBG, G_7, G_{20} and $Dext_{34}$, respectively, using centrifugal filtration (PES and cellulose membrane materials).

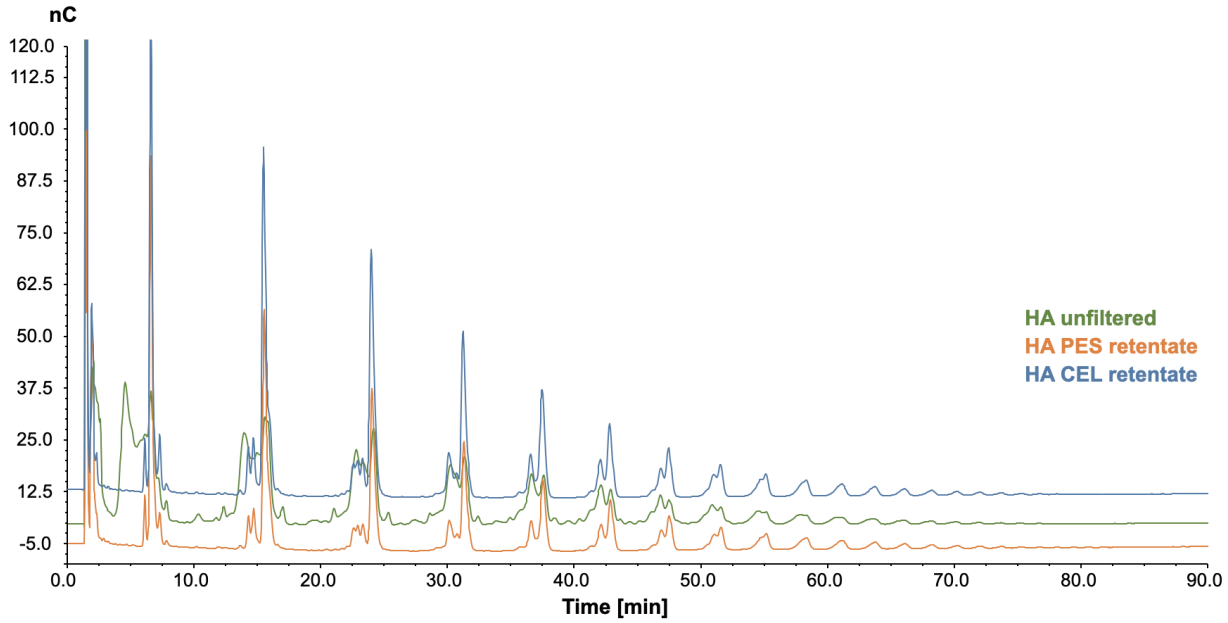

Figure A.1: HPAEC-PAD chromatograph of unpurified and purified acid hydrolyzed HA (1 mg/mL, DP around 10) using centrifugal filtration. CEL and PES refers to cellulose and PES membrane material, respectively.

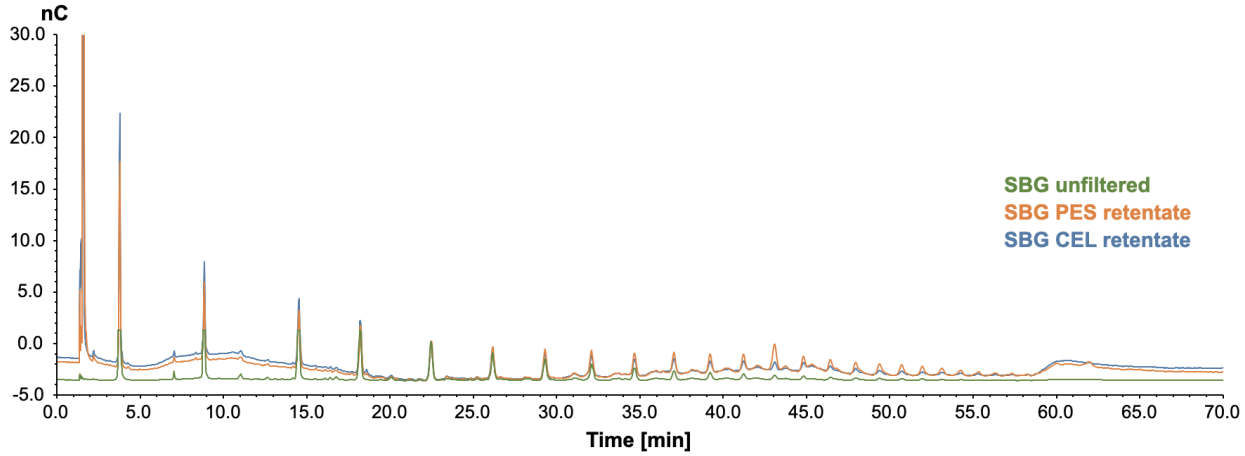

Figure A.2: HPAEC-PAD chromatograph of unpurified and purified acid hydrolyzed SBG (1 mg/mL, DP around 10) using centrifugal filtration. CEL and PES refers to cellulose and PES membrane material, respectively.

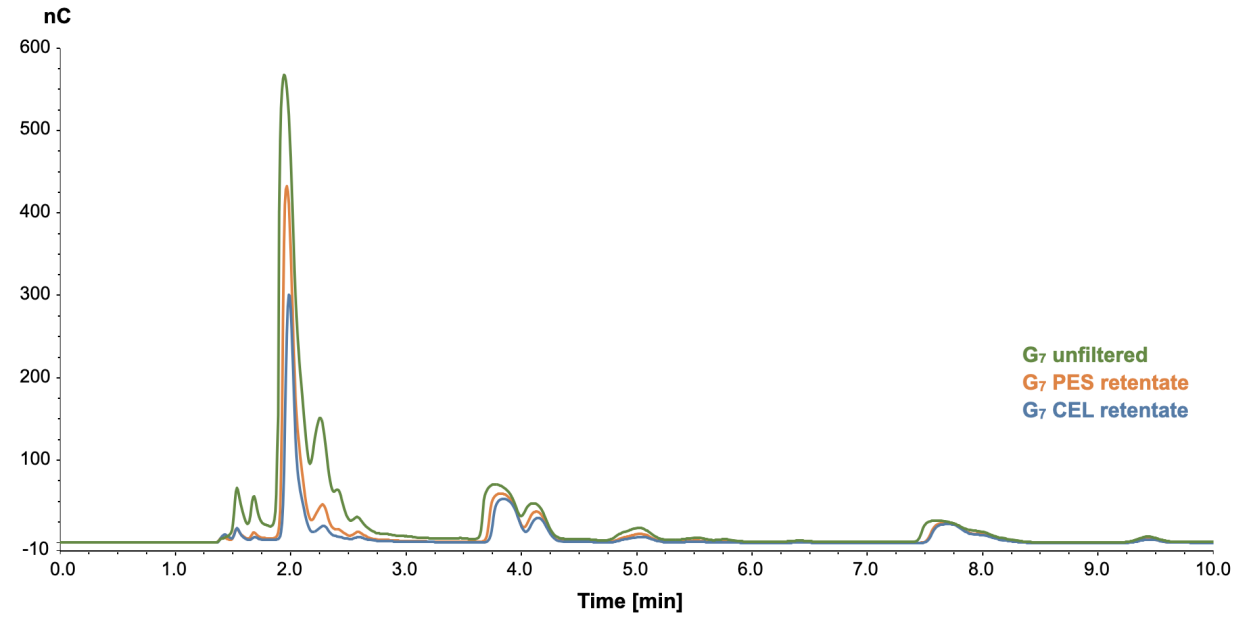

Figure A.3: HPAEC-PAD chromatograph of unpurified and purified G_7 (1 mg/mL) using centrifugal filtration. CEL and PES refers to cellulose and PES membrane material, respectively.

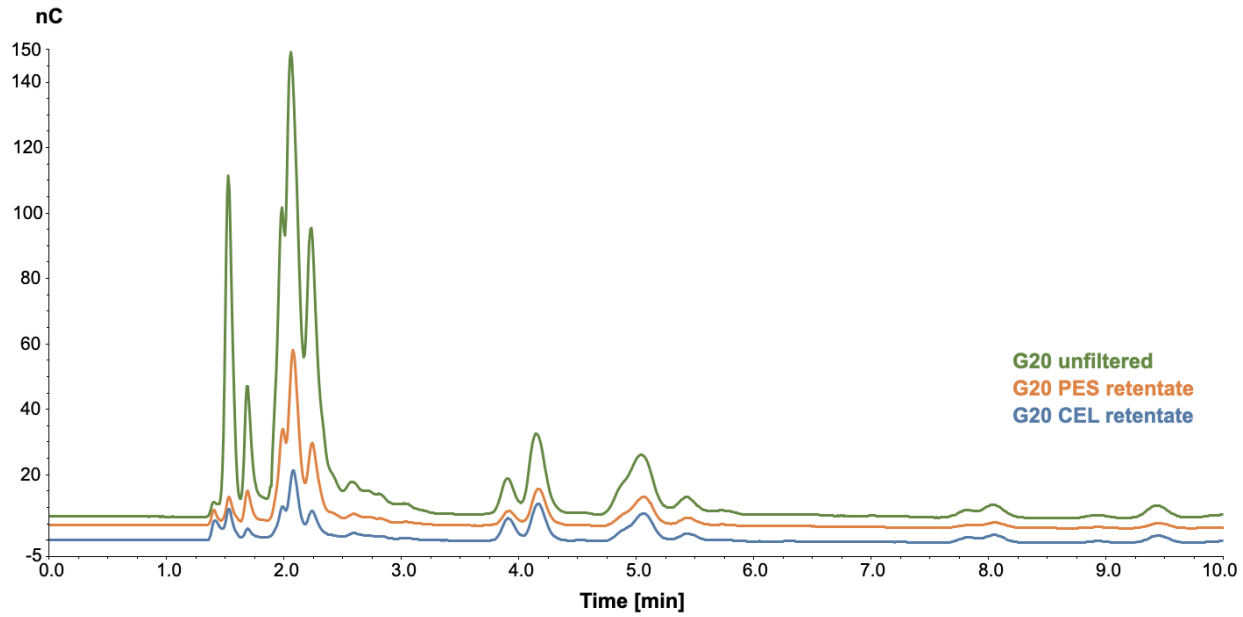

Figure A.4: HPAEC-PAD chromatograph of unpurified and purified G_{20} (1 mg/mL) using centrifugal filtration. CEL and PES refers to cellulose and PES membrane material, respectively.

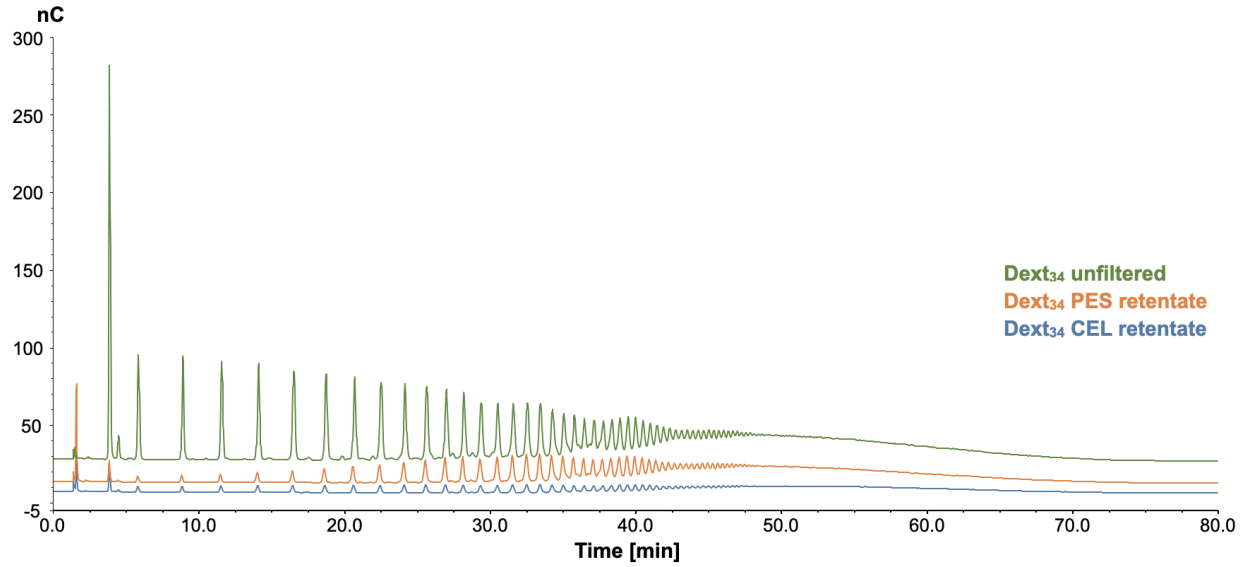

Figure A.5: HPAEC-PAD chromatograph of unpurified and purified $Dext_{34}$ (1 mg/mL) using centrifugal filtration. CEL and PES refers to cellulose and PES membrane material, respectively.

B Additional NMR spectra

A detailed ^{1}H-NMR spectrum showing the contaminants glycerol and isopropanol present in the D_5M sample, as well as reference spectra, is presented in Figure B.1. Figure B.2 shows the integrated ^{1}H-NMR spectra of purified D_5M and $D_{10}M$ used to calculate the yield. Further, a ^{1}H-NMR spectrum of the in-house D_5M sample prepared by Jesper E. Pedersen (Department of Biotechnology, NTNU) used in the chitin-*b*-chitosan diblock preparation, is shown in Figure B.3. Figure 4.4.3 compares the ^{1}H-NMR spectra of D_5M, A_4M-PDHA and A_4M-*b*-MD_5. The ^{1}H-NMR spectrum of pure PDHA is shown in Figure B.4.

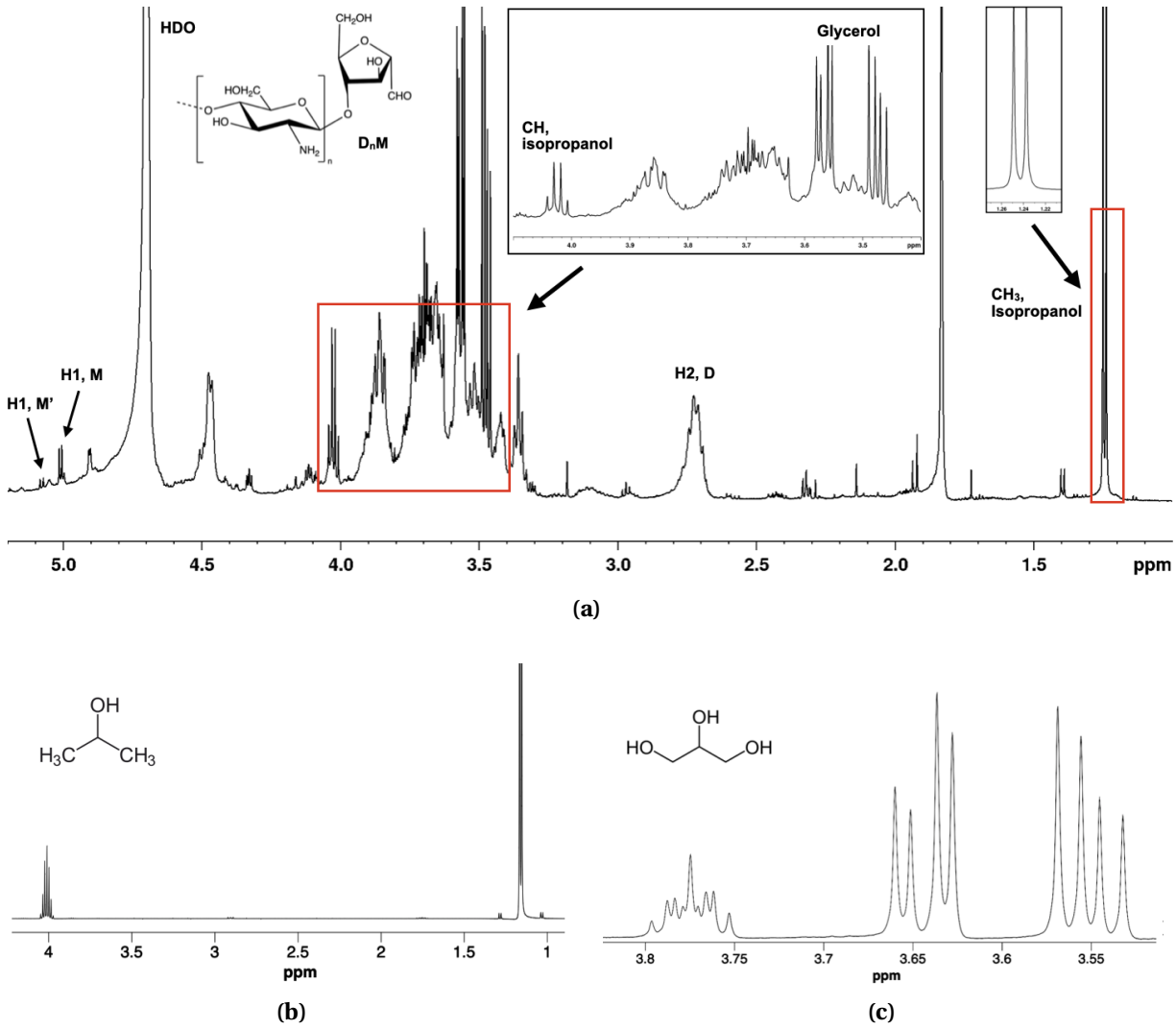

Figure B.1: ^{1}H-NMR spectra of **(a)** D_5M (600MHz, RT, D_2O) from the chromatogram in Figure 4.2.1a (assumed DP of 6), **(b)** isopropanol (500 MHz, RT, H_2O) [8] and **(c)** glycerol (500 MHz, RT, H_2O) [7]. The spectra are annotated according to literature [43,41].

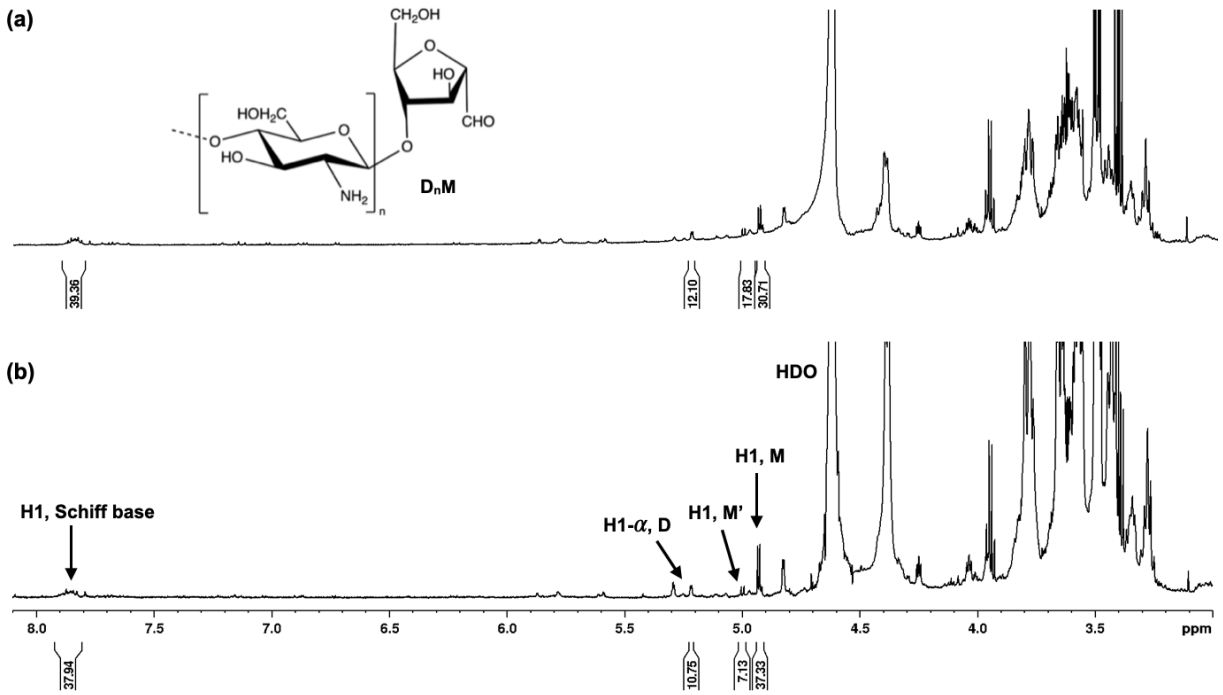

Figure B.2: Integrated ^{1}H-NMR spectra (600MHz, RT, D_2O) of **(a)** D_5M and **(b)** $D_{10}M$ (fractions with assumed DP 6 and 11, respectively, from the chromatogram in Figure 4.2.1a). The spectra are annotated according to literature [12,43].

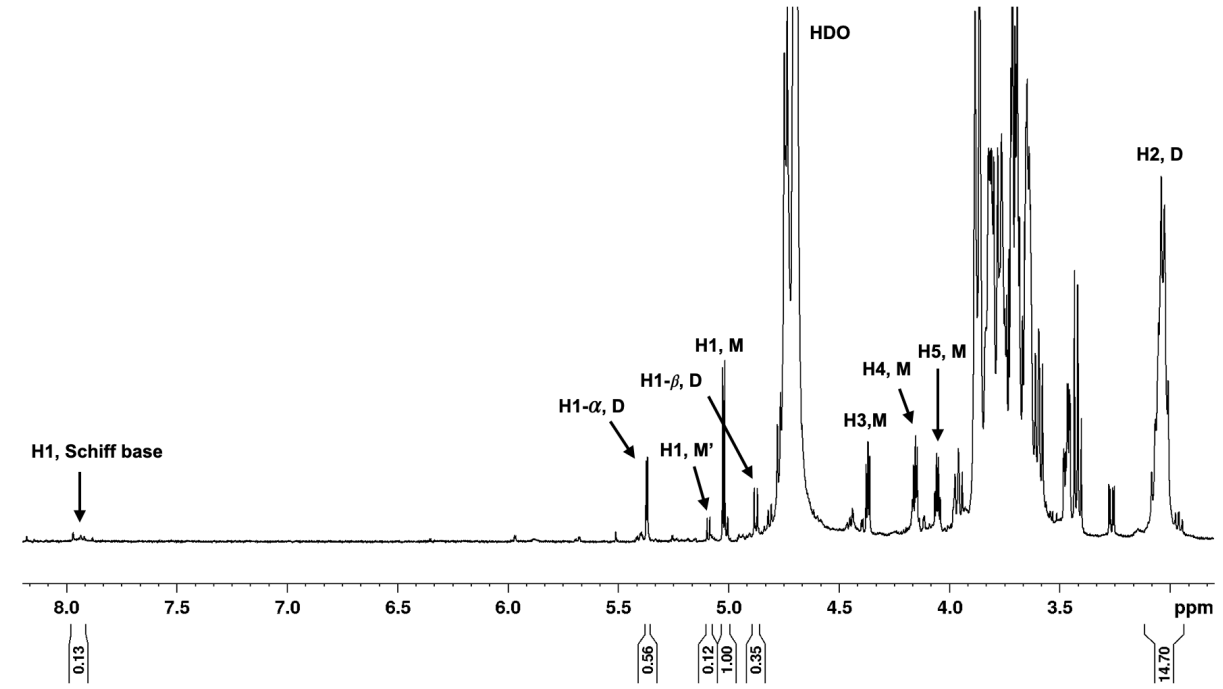

Figure B.3: Integrated ^{1}H-NMR spectrum (600MHz, RT, D_2O) of in-house D_5M prepared by Jesper E. Pedersen (Department of Biotechnology, NTNU). The spectra are annotated according to literature [12,43].

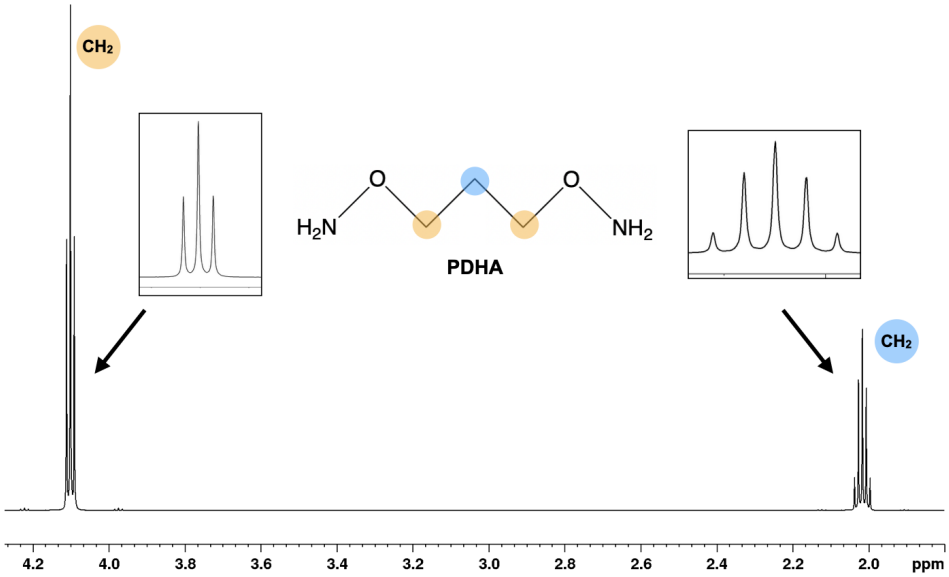

Figure B.4: ^{1}H-NMR spectra (600MHz, RT, D_2O) of pure PDHA.

C Preparation of D_nM: protocol discrepancies

C.1 Preparation and fractionation

Figure C.1 illustrates the preparation of batch 1, 2 and a control batch of D_nM oligomers, whereas Figure C.2 show the corresponding SEC chromatograms.

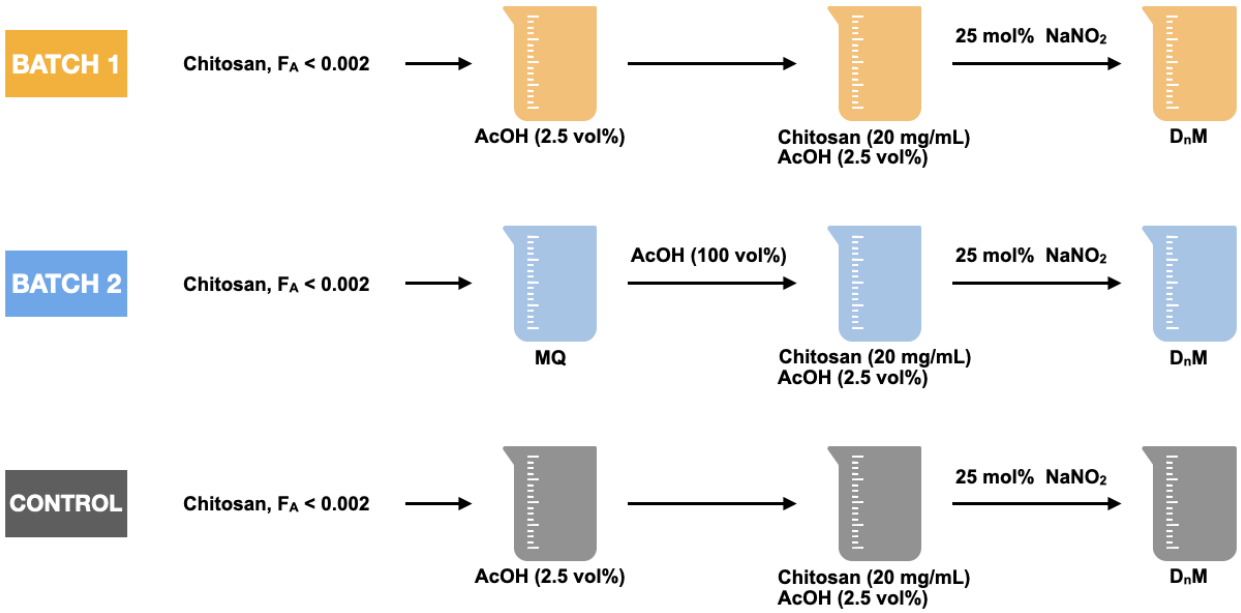

Figure C.1: Overview of the preparation of D_nM oligomers: batch 1, batch 2, and a control batch.

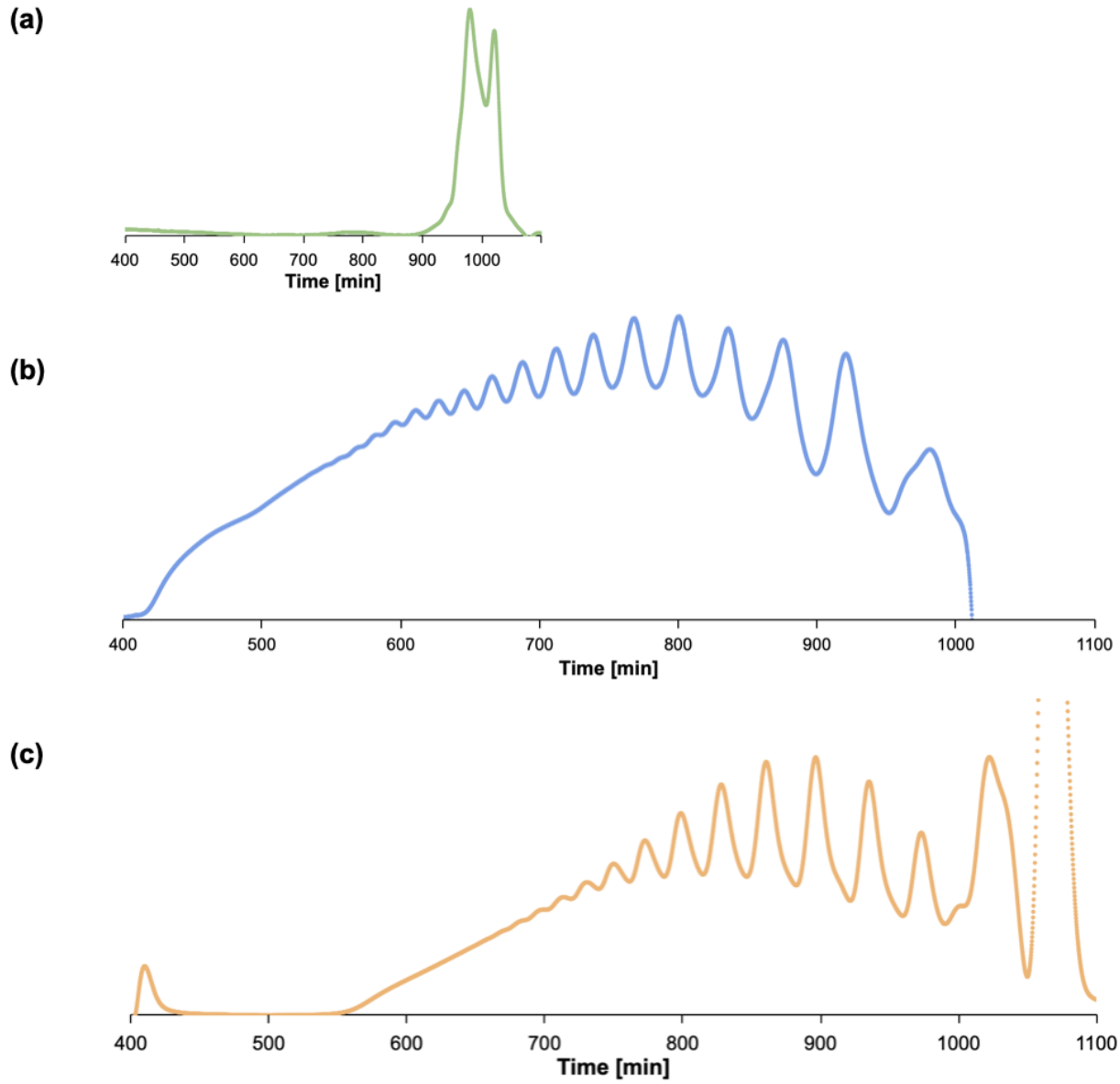

Figure C.2: SEC chromatogram of **(a)** batch 2, **(b)** batch 1 and a **(c)** control batch of DnM oligomers prepared as illustrated in Figure C.1. SEC-system 1 was used, and the injection samples were 10 mg, 180 mg and 50 mg for **(a)**, **(b)** and **(c)**, respectively.

C.2 Calculations on chitosan degradation by AcOH

Calculations on the possible chitosan degradation by AcOH (100%) in batch 2 are presented here. The degradation rate constant as a function of HCl concentration for chitosan (F_A = 0.62) at 60°C is shown in Figure C.3, and was acquired from Vårum *et al.*[48]. To determine the HCl concentration equivalent to the localized AcOH concentration, Equations (C.1) and (C.2) were used, in which 100% AcOH is equivalent to 0.02 M HCl. Further, random depolymerization of linear polymers can be described by Equation (C.3), where M_n is the number average molecular weight at t; M_{n0} is the number average molecular weight at t=0; M_0 is the monomer molecular weight; k is the degradation rate constant; and t is the degradation time. To determine the change in DP caused by acid depolymerization, $k_{A-D} = 5.0 \cdot 10^{-8}$ (Figure C.3, 0.02 M HCl), M_0 = 197.5 Da and M_n was estimated to be 200 kDa. The results are presented in Table C.1.

Table C.1: Theoretical decrease in DP as a result of chitosan (F_A=0.002) depolymerization by AcOH (100%). The degradation rate, k_{A-D}, is $5.0 \cdot 10^{-8}$

Time [s]	0	2	10	30	60	180
Decrease in DP [%]	0	0.01	0.04	0.10	0.15	0.60

$$AcOH \rightleftharpoons AcO^- + H^+ \tag{C.1}$$

$$K_a = \frac{[AcO^-][H^+]}{[AcOH]} \tag{C.2}$$

$$\frac{1}{M_n} = \frac{1}{M_{n0}} + \frac{k}{M_0} t \tag{C.3}$$

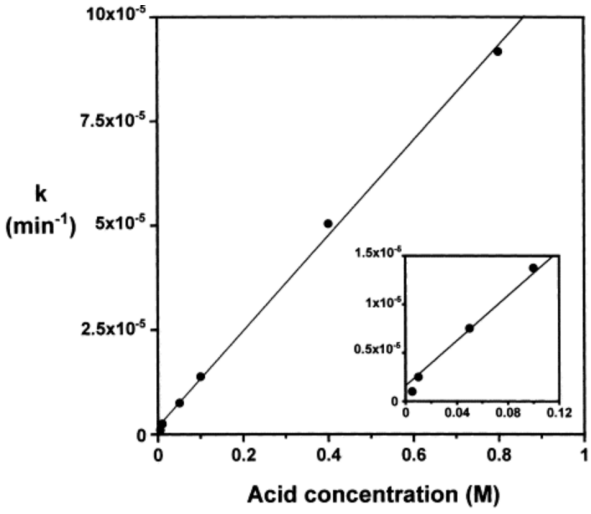

Figure C.3: Degradation rate constants as a function of HCl concentration for chitosan determined by a viscosity assay of chitosan (F_A = 0.62, 1.5 mg/mL) in 0.4M HCl at 60°C. Figure acquired from Vårum *et al.*[48].

D Suggested optimized protocol for chitin-*b*-chitosan diblocks

An optimized protocol for preparation of A_nM-PDHA-MD_m diblocks is suggested here, but has not been tested due to time limitations. The protocol is divided into three main steps: preparation of A_nM- and D_nM oligomers, preparation of D_nM-PDHA conjugates using a two-pot procedure, and preparation of the diblock.

A_nM- and D_nM oligomers

Chitosan (20 mg/mL, F_A=0.48 and F_A=0.002 for A_nM and D_nM, respectively) is dissolved in degassed MQ water containing AcOH (2.5 vol%) for 15-20 min using N_2, and left on a magnetic stirrer at RT until homogeneous. The polymer solutions are cooled to 4°C, along with degassed $NaNO_2$ solutions (20 mg/mL, 1.3 and 0.25 molar ratio to D-units for A_nM and DnM, respectively). Lastly, the cool $NaNO_2$ solutions are added to their respective chitosan solutions, and left on a magnetic stirrer overnight in the dark at 4°C. After degradation, the theoretical DPs are < 10.

Further, the A_nM degradation mixture is centrifuged and the pellet is washed with AcOH (2.5 vol%) three times to remove insoluble chitin oligomers. The supernatant is filtered (2.7 and 0.7 µm) and fractionated using SEC (0.15 M AmAc buffer, pH 4.5). Pooled fractions are purified by dialysis (MWCO = 100-500 Da) and freeze-dried. The D_nM degradation mixture is directly freeze-dried prior to subsequent conjugation.

D_nM-PDHA conjugates

Unfractionated D_nM oligomers (7-10 mM) is conjugated with 10x PDHA in NaAc buffer (pH 4.0, RT) for 5-6 hours, and reduced with 20x PB for 48h at 40°C. The reduction is terminated by dialysis (MWCO = 100-500 Da) against NaCl (0.05 M) until the remaining PB has dissolved, followed by MQ-water until the conductivity is < 2µS/cm. The dialysis water should be pH adjusted to 4.5 to avoid potential precipitation. Subsequently, the reaction mixture is fractionated by SEC (0.15 M AmAc, pH 4.5), in which pooled fractions are purified by freeze-drying to reduce loss of material. By conjugating PDHA to D_nM prior to freeze-drying, the M residue is protected against Schiff base reactions.

A_nM-*b*-MD_m diblocks

A_nM and D_mM-PDHA are prepared as described for D_nM-PDHA, however, here in equimolar ratios. Reacted and unreacted conjugates are separated by SEC fractionation (0.15 M AmAc, pH 4.5), and freeze-dried directly.

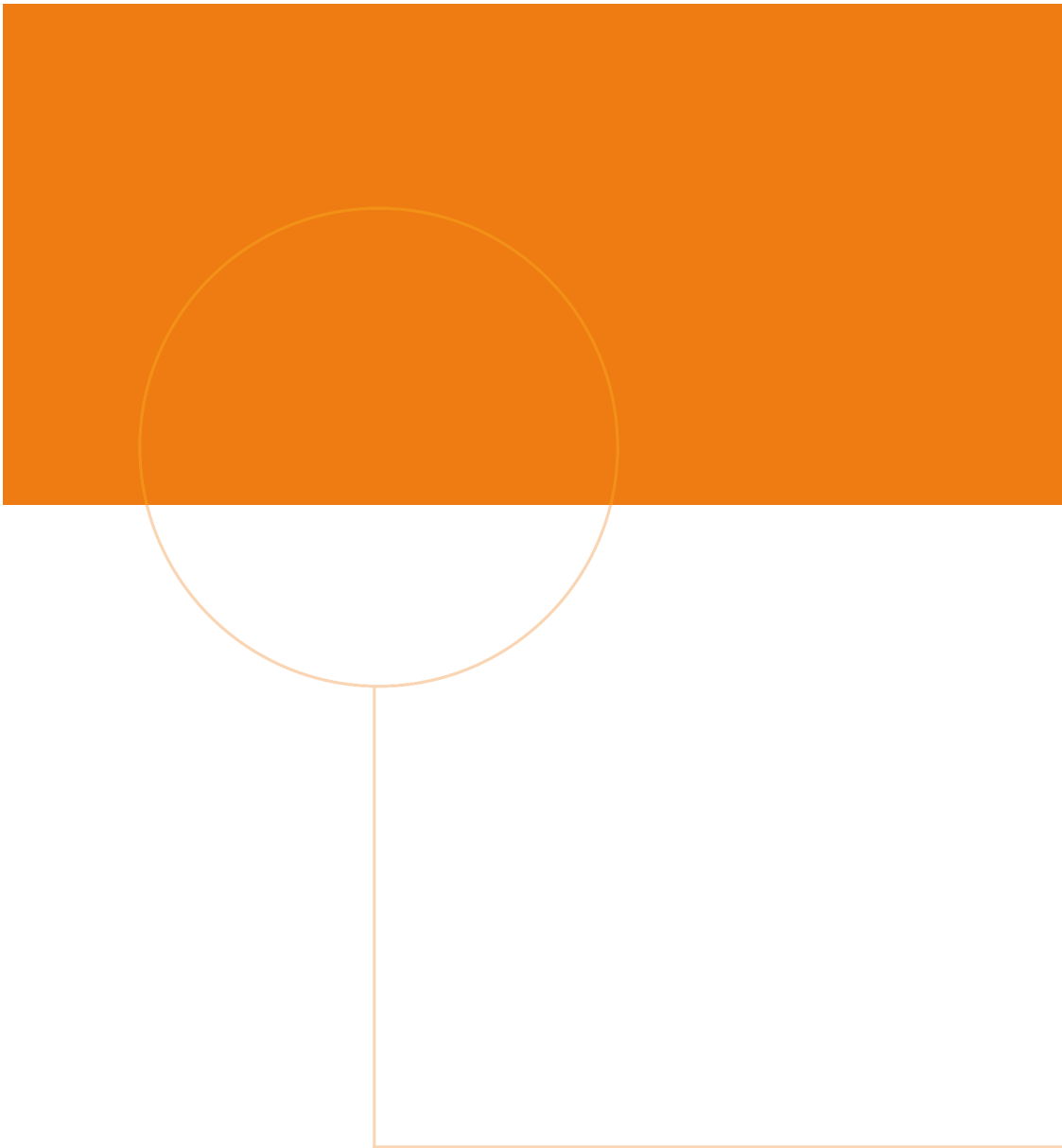

NTNU

Norwegian University of
Science and Technology